Interpreting eddy fluxes

Carsten Eden[1], Richard J. Greatbatch[2] and Dirk Olbers[3]

[1] *Leibniz–Institut für Meereswissenschaften, IFM–GEOMAR, Kiel, Germany*

[2] *Department of Oceanography, Dalhousie University, Halifax, Canada*

[3] *Alfred Wegener Institute for Polar and Marine Research, Bremerhaven, Germany*

Manuscript re–submitted to JPO, 24. May 2005.

Corresponding author address:
Carsten Eden
IFM–GEOMAR,
FB I, Ocean circulation and climate dynamics
Düsternbrooker Weg 20
24105 Kiel, Germany
email: ceden@ifm-geomar.de

All figures are available in electronic format.

Abstract

Consistent ways of interpreting eddy buoyancy fluxes averaged at constant height are presented and compared with previous interpretations, in particular the Transformed Eulerian Mean (TEM) of Andrews and McIntyre (1978), and the Temporal Residual Mean (TRM) of McDougall and McIntosh (1996). The previous decompositions imply eddy–induced diapycnal mixing related to local cross–isopycnal eddy fluxes that may not be physically justified. In particular, this diapycnal mixing is not necessarily vanishing for adiabatic and steady flow and can become large (compared to the mean diabatic forcing) for weakly diabatic flow as revealed in numerical simulations.

We introduce a consistent version of the TEM that leads by construction to a residual streamfunction with minimal eddy–induced diapycnal diffusion, which is related to the integrated diabatic forcing of the domain and which vanishes for adiabatic and steady flow. This is achieved by subtracting an optimal rotational component from the eddy tracer fluxes found from the solution of a minimization. Consideration of the full hierarchy of tracer moments and generalizing ideas reaching back to Marshall and Shutts (1981) yields a TRM version with eddy–induced (or enhanced) diapycnal diffusion in the steady case only if there are local covariances between the diabatic forcing and the tracer. In contrast to McDougall and McIntosh's version of TRM, the new, consistent version can be evaluated for any stratification and to any order in perturbation amplitude. It is shown that all the new flux decompositions collapse to a single, consistent one in the adiabatic and steady case, giving also well–defined boundary conditions for the residual streamfunction.

1 Introduction

The Boussinesq form of the conservation equation for a tracer with concentration b in the ocean (or the atmosphere) is given by

$$\frac{\partial b}{\partial t} + \nabla \cdot (\mathbf{u} b) = Q \tag{1}$$

where $\mathbf{u}$ denotes the instantaneous, three-dimensional velocity and Q a forcing term. Both the ocean and atmosphere are turbulent fluids, full of "rapidly evolving perturbations" (eddies) on a "slowly evolving mean state". The presence of the eddies means that the instantaneous tracer distribution is often of little interest; instead, it is the dynamics and evolution of an "averaged"

state which is important. This, in turn, requires the definition of an average or filter with which to view the dynamics and evolution of the tracer field, and which, in turn, determines what is meant by "rapid", "slow" and "mean state".

A simple example is the zonal mean; that is b, $\mathbf{u}$ and Q are decomposed into zonal averages at constant height and deviations from that average:

$$\bar{b} = (x_2 - x_1)^{-1} \int_{x_1}^{x_2} b \; dx \quad , \quad b' = b - \bar{b} \tag{2}$$

and correspondingly for $\mathbf{u}$ and Q. Substituting the decomposition given by Eq. (2) into the instantaneous tracer budget and averaging the result leads to the equation for the mean tracer $\bar{b}$ given by

$$\frac{\partial \bar{b}}{\partial t} + \nabla \cdot (\bar{\mathbf{u}}\bar{b}) + \nabla \cdot (\overline{\mathbf{u}'b'}) \;\; = \;\; \bar{Q} \tag{3}$$

An immediate difficulty is presented by the "eddy tracer fluxes"[1] $\overline{\mathbf{u}'b'}$. These fluxes couple the mean tracer budget to that of the perturbations, such that the evolution of the perturbations has to be known to predict the mean tracer. Of course, the solution to this problem is thought to be given by "parameterizing" the perturbation quantities in terms of the mean quantities. However, before parameterizing the effect of the eddy tracer fluxes, it is necessary to understand and interpret them. Understanding and interpreting the eddy fluxes is the focus of the present paper.

Some insight into the nature of the eddy tracer fluxes can be obtained by considering a layered framework, in which instantaneous contours of b are taken as layer interfaces. In the continuous limit of infinitesimal layer thickness, this is the same as using b as the vertical coordinate[2]. Taking b to be potential density[3] then corresponds to using "isopycnal coordinates" (e.g. McDougall (1987)). Since the interior oceanic flow is almost adiabatic (Wüst, 1935), the diabatic forcing Q is expected to be small in the ocean interior and to be associated with weak diapycnal mixing. In the limit of vanishing instantaneous forcing Q, there is no instantaneous exchange of b across layers (isopycnals) and it is easy to see that in the isopycnally-averaged budget for b there can be no cross-isopycnal flux. Furthermore, the mean forcing (related to Q) is controlling the cross-isopycnal flux in the mean budget of the layer thickness.

[1] Note that the vectors $\bar{\mathbf{u}}$, $\mathbf{u}'$, the operator ∇ and correspondingly the fluxes $\bar{\mathbf{u}}\bar{b}$ and $\overline{\mathbf{u}'b'}$ in Eq. (2) and in the following section are two dimensional, that is their zonal component vanishes.

[2] Assuming that b is a monotonic function of depth. See Nakamura (2001) and Nurser and Lee (2004) for a generalization of this approach for non–monotonic functional forms of b.

[3] Note that we assume for simplicity an equation of state in which potential density and neutral density are the same.

Returning to z–coordinates, this property of the eddy fluxes is not as obvious. In fact, eddy tracer fluxes averaged at constant height (instead of at constant b) usually show strong diapycnal components even for the steady, weakly diabatic case, suggesting strong eddy–induced diapycnal processes as we shall show below. On the other hand, z–coordinates are convenient and simple to use for both analytical considerations and numerical calculations. In fact, an overwhelming number of analytical and numerical models are based on z–coordinates, rather than layered or isopycnal coordinates. Therefore, it would be desirable if the character of eddy tracer fluxes as revealed above in the layered framework could be carried over to the mean tracer budget in z–coordinates. Based on these considerations, we can formulate the following statement, which we would like to apply in z-coordinates:

i) If there is no instantaneous diabatic forcing, Q, there should be no diabatic effects in the mean budget for b. As a consequence, the divergence of the eddy tracer flux must be entirely expressible as a divergence of an advective flux of the mean tracer.

Statement i) is a feature of the eddy tracer flux parameterization of Gent et al. (1995) (the so-called Gent and McWilliams (GM) parameterization). In GM, the eddy fluxes are assumed to be adiabatic in their effect, and consequently, the parameterization is written entirely in terms of an advective velocity. Although this is certainly a reasonable first order approximation, Radko and Marshall (2004) have raised the possibility that eddy-induced diapycnal mixing, especially in association with the surface and bottom boundary layers (where diabatic effects are relatively strong) might be important in the dynamics of the large-scale ocean circulation. In particular, their work implies that eddy fluxes do indeed have a diabatic component, with the implication that a parameterization of the eddy tracer flux should include a diabatic component as well. Tandon and Garrett (1996) had earlier pointed out that the release of available potential energy from the mean state that is implied by the GM parameterization must, in turn, be dissipated in some way. These authors argue that the dissipation implies significant diapycnal mixing in association with eddies, and they point out the likely importance of the surface and bottom boundary layers, especially air-sea interaction at the surface, in accounting for this dissipation.

In fact, the diabatic nature of the eddy fluxes can also be understood in an integral sense in z–coordinates as outlined by Radko and Marshall (2004). Consider an integral over an area A (or volume for the three–dimensional case and temporal averaging) above a mean isopycnal $\bar{b}(y,z) = const$ of the mean tracer budget Eq. (3)

$$\int_A dA(\nabla \cdot (\bar{\mathbf{u}}\bar{b}) + \nabla \cdot (\overline{\mathbf{u}'b'})) = \int_A dA(\bar{Q} - \frac{\partial}{\partial t}\bar{b}) \tag{4}$$

Using Gauss' divergence theorem and the no flow boundary conditions for the mean and the eddy tracer fluxes at the northern and southern lateral boundaries of the channel and the surface, it is clear that only the eddy flux across the mean isopycnal $\bar{b} = const$ remains from the mean and eddy advection in the integral balance:

$$\int_{s_0}^{s_1} \overline{\mathbf{u}'b'} \cdot \mathbf{n}\, ds = \int_A dA(\bar{Q} - \frac{\partial}{\partial t}\bar{b}) \tag{5}$$

where the vector $\mathbf{n} = \nabla\bar{b}|\nabla\bar{b}|^{-1}$ points perpendicular to the mean isopycnal $\bar{b} = const$ and s denotes a coordinate along the mean isopycnal from s_0 at the southern end of the channel to s_1 at the northern end of the channel. This means that if the integral on the right hand side of the integral balance vanishes, i. e. if the mean diapycnal forcing $\bar{Q}$ vanishes in quasi–steady state[4], the integrated diapycnal eddy flux across that mean isopycnal must also vanish. Eq. (5) therefore yields an integral constraint for averaging in z–coordinates, similar to the previous one averaging in isopycnal coordinates. The difference is that the constraint in z–coordinates holds only in a (weaker) integral sense while in isopycnal coordinates the constraint holds also locally. That means that statement i), which is implicitly assumed in the GM parameterization and which was deduced from the isopycnal framework and applied to z–coordinates, carries over the weaker integral constraint to a (stronger) local one in z–coordinates.

The way we shall implement statement i) in this paper is by including rotational fluxes in an eddy flux decomposition into advective and diffusive parts, similar to the flux decompositions of Andrews and McIntyre (1978) and McDougall and McIntosh (1996). As examples of the performance of our eddy flux interpretation we diagnose numerical experiments, which are presented in section 2. In section 3, we review the classical flux decomposition by Andrews and McIntyre (1978), the Transformed Eulerian Mean (TEM) method, and diagnose it in the numerical experiments. While the original TEM is shown to be inconsistent with statement i), Sections 4 and 5 present consistent TEM versions in this respect. In section 6 and 7 we discuss and apply to the model consistent generalizations of the eddy flux interpretations of Marshall and Shutts (1981); McDougall and McIntosh (1996) and Medvedev and Greatbatch (2004) while section 8 concludes and discusses the results.

[4] We mean by quasi–steady state that $\frac{\partial\bar{b}}{\partial t} = 0$ but $\frac{\partial b'}{\partial t} \neq 0$.

2 Numerical simulations of eddy fluxes

We are diagnosing numerical experiments using an OGCM in several idealized configurations with respect to the above presented eddy flux decompositions. The numerical code[5] which is used to integrate the OGCM is based on a revised version of MOM2 (Pacanowski, 1995) and formulated in z–coordinates.

Experiment CHANNEL-3 is a setup with a reentrant channel on a β–plane (referenced to the southernmost latitude of the model domain). Horizontal resolution is $1/3^o$ and there are 20 levels of 100m thickness. Initial conditions are a state of rest and constant meridional and vertical gradients in temperature ($-1 \times 10^{-5} K/m$ and $8.2 \times 10^{-3} K/m$ respectively) and no zonal gradient (except for a small perturbation). A linear equation of state is used ($\partial\rho/\partial T = -0.2 \times 10^{-3} kg/m^3/K$) and salinity set to a constant. Boundary conditions are no slip at the side walls and vanishing heat fluxes at the side walls, surface and bottom boundaries (the detailed boundary conditions for heat are examined below). Bottom friction following a quadratic drag law is used with a coefficient of 1.5×10^3, lateral biharmonic friction with viscosity of $2 \times 10^{11} m^4/s$ and the Quicker advection scheme (Leonard, 1979) for the tracer with no explicit diffusion. Explicit vertical viscosity is $2 \times 10^{-4} m^2/s$. Temperature at the three northernmost and southernmost grid points is relaxed towards the initial condition with a timescale ranging from 3 days at the boundary to 15 days at the outer edge of the relaxation zone.

Two further experiments are discussed in which we aim to reduce the interior diabatic forcing. Since we use no explicit diffusion in all model runs, the diabatic forcing outside the relaxation zones is due to implicit (numerical) diffusion by the advection scheme (Quicker) and other spurious numerical effects (Griffies et al., 2000; Eden and Oschlies, 2005). The most effective way to reduce these effects and correspondingly Q in the model is simply given by increasing the resolution. In experiment CHANNEL-6 (CHANNEL-12) the horizontal and vertical model resolution was increased by a factor 2 (4). In addition, the biharmonic viscosity was decreased to $1 \times 10^{11} m^4/s$ ($2 \times 10^{10} m^4/s$) and the temperature is relaxed towards the initial condition in 6 (12) southern– and northernmost grid points. All other aspects of the model are unchanged with respect to experiment CHANNEL-3.

After a couple of weeks integration time, baroclinic instability sets in and is producing large zonal deviations of the flow in the channel in all experiments. Figure 1 shows the fully developed stage of turbulence after one year integration in CHANNEL-3. In all experiments, the model

[5]The numerical code together with all configurations used in this study can be accessed at *http://www.ifm.uni-kiel.de/fb/fb1/tm/data/pers/ceden/spflame/index.html*.

is integrated for 40 years and temporal and zonal averages are taken for the last 30 years of the integration. In the following we relate b to temperature, i. e. density, since temperature acts as the only (active) tracer in the model.

3 The classical eddy flux decompositions

In this section we review several ways of interpreting the eddy tracer flux resulting from zonal averaging at constant height. They are complemented in the next sections with new approaches for the interpretation of eddy tracer flux. Note that all results carry over to temporal averaging in three dimensions. Note also that in the sections concerning the zonal mean problem we use the following notation (Hasselmann, 1982)

$$\nabla\alpha = \begin{pmatrix} \alpha_y \\ \alpha_z \end{pmatrix} \quad \text{and} \quad \underset{\neg}{\nabla}\alpha = \begin{pmatrix} -\alpha_z \\ \alpha_y \end{pmatrix} \tag{6}$$

where the subscripts y and z denote differentiation of the scalar α in the meridional and vertical direction, respectively, and the vector subscript $\neg$ anti–clockwise rotation by 90^o.

The Transformed Eulerian Mean method of Andrews and McIntyre (1976) (TEM-I hereafter) introduces a decomposition of the eddy tracer flux $\mathbf{F}$ into a part aligned along contours of $\bar{b}$ and a correction term

$$\mathbf{F} = \begin{pmatrix} \overline{v'b'} \\ \overline{w'b'} \end{pmatrix} = B\ \underset{\neg}{\nabla}\bar{b} + \delta \mathbf{e}^{(z)}. \tag{7}$$

Here, the ad hoc choice $B = -\overline{v'b'}/\bar{b}_z$ yields a streamfunction for an eddy–induced tracer advection velocity $\mathbf{u}_{eddy} = -\ \underset{\neg}{\nabla}B$ and $\delta = \overline{v'b'}\bar{b}_y/\bar{b}_z + \overline{w'b'}$. Substituting this expression for $\mathbf{F}$ into the mean tracer budget (Eq. (3)) yields

$$\bar{b}_t + (\bar{\mathbf{u}} - \ \underset{\neg}{\nabla}B) \cdot \nabla\bar{b} \ \ = \ \ \bar{Q} - \delta_z \tag{8}$$

In general, the remainder $\delta = \overline{v'b'}\,\bar{b}_y/\bar{b}_z + \overline{w'b'}$ is not zero; only if the eddy flux $\mathbf{F}$ is entirely along contours of $\bar{b}$ does the remainder δ vanish. In this limit, the effect of $\nabla \cdot \mathbf{F}$ can be represented by the eddy–induced tracer advection velocity $\mathbf{u}_{eddy}$, which together with the mean velocity $\bar{\mathbf{u}}$ advects the tracer $\bar{b}$. The sum $\mathbf{u}_{eddy} + \bar{\mathbf{u}}$ is sometimes called the "residual velocity". For $\mathbf{F} \cdot \nabla\bar{b} \neq 0$, the remainder δ can become small assuming $|\bar{b}_y| << |\bar{b}_z|$ and accordingly $|\overline{w'b'}| << |\overline{v'b'}|$, i. e. a strongly stratified situation, taking b to be density.

The alternative TEM flux decomposition of Held and Schneider (1999) (TEM-II hereafter) uses the vertical eddy fluxes to construct a streamfunction for the eddy–induced velocity:

$$\mathbf{F} = B \; \underset{\neg}{\nabla}\bar{b} + \eta \mathbf{e}^{(y)} \quad , \quad \bar{b}_t + (\bar{\mathbf{u}} - \; \underset{\neg}{\nabla} B) \cdot \nabla \bar{b} \;\; = \;\; \bar{Q} - \eta_y \tag{9}$$

where $B = \overline{w'b'}/\bar{b}_y$ and $\eta = \overline{w'b'}\,\bar{b}_z/\bar{b}_y + \overline{v'b'}$. The remainder η is again zero if the eddy flux has no component across contours of $\bar{b}$ and can become small if $|\bar{b}_y| >> |\bar{b}_z|$ and $|\overline{v'b'}| << |\overline{w'b'}|$, e. g. in the oceanic mixed layer, for $\mathbf{F} \cdot \nabla \bar{b} \neq 0$.

It is, however, possible and more elegant to combine the TEM-I and TEM-II in the following way. We decompose the eddy tracer flux in directions along and across contours of $\bar{b}$

$$\mathbf{F} \;\; = \;\; B \; \underset{\neg}{\nabla}\bar{b} - K \nabla \bar{b} \tag{10}$$

where B and K are given by projections of the eddy flux along and across contours of $\bar{b}$ respectively

$$B \;\; = \;\; |\nabla \bar{b}|^{-1} F_{\perp} \quad , \quad K = -|\nabla \bar{b}|^{-1} F_{||} \tag{11}$$

with $F_{\perp} = \overline{\mathbf{u}'b'} \cdot \mathbf{n}$ the cross–isopycnal component of the eddy tracer fluxes, $F_{||} = \overline{\mathbf{u}'b'} \cdot \mathbf{s}$ the along–isopycnal component of the eddy tracer fluxes, and $\mathbf{s} = |\; \underset{\neg}{\nabla}\bar{b}|^{-1} \nabla \bar{b}$ is the unit vector along the $\bar{b}$-contours.

Such a decomposition (TEM-G hereafter) can be found in Andrews and McIntyre (1978) and is used for instance by Nakamura (2001), Greatbatch (2001) and Olbers and Visbeck (2005). Note that B is again a streamfunction for the eddy–induced advection velocity. In addition, an eddy–induced diffusion term with diffusivity K shows up in the mean tracer budget

$$\bar{b}_t + (\bar{\mathbf{u}} - \; \underset{\neg}{\nabla} B) \cdot \nabla \bar{b} \;\; = \;\; \bar{Q} + \nabla \cdot K \nabla \bar{b} \tag{12}$$

The eddy–induced diapycnal diffusivity K vanishes for $\mathbf{F} \cdot \nabla \bar{b} = 0$ (as for the remainder δ and η in the TEM-I and TEM-II cases). In the limits $|\bar{b}_y| >> |\bar{b}_z|$ or $|\bar{b}_y| << |\bar{b}_z|$ the streamfunction B converges to that in the TEM-II or TEM-I cases, respectively. Likewise, in these limits, the eddy–induced diapycnal diffusivity K becomes similar to $\eta/\bar{b}_y$ or $\delta/\bar{b}_z$, respectively. This feature makes the TEM-G flux decomposition useful for the more general situation and especially for the transition regions between the ocean interior and the surface and bottom boundary layers (see also Plumb and Ferrari (2005)). Furthermore, the form of a diapycnal diffusivity K, rather than the remainder terms δ or η, offers a convenient way to quantify the effect of the remainder in comparison with explicit diapycnal diffusivities specified in the numerical experiments, and our knowledge of diapycnal diffusivities in the ocean.

Fig. 2 (a) shows the (residual) streamfunction for the total flow, $(\bar{\mathbf{u}} - \underset{\neg}{\nabla} B)$, for TEM-G in experiment CHANNEL-3. The value for the residual streamfunction ranges from 0 to $-30\,m^2/s$. Note that the streamfunction is given for the zonally averaged flow and that a value of $30\,m^2/s$ corresponds to about $30\,Sv$ per 10^o longitude volume transport in this model setup. The streamfunction of the Eulerian mean flow in CHANNEL-3 ($-\underset{\neg}{\nabla} B_m = \bar{\mathbf{u}}$, not shown explicitly) in the interior channel is much smaller (only up to $3\,m^2/s$) than the eddy streamfunction B, only in the restoring zones the mean streamfunction reaches values comparable to the eddy driven streamfunction. Thus, the meridional overturning in the interior of the channel is dominantly eddy–driven in this setup. Note that in addition to the meridional overturning, there is a strong zonal transport of about $400\,Sv$ (not shown). Note also that in this setup the TEM-I version of Andrews and McIntyre (1976) is virtually the same as TEM-G since $|b_y| << |b_z|$, while TEM-II differs a lot from TEM-G.

The residual streamfunction for TEM-G (Fig. 2 a) shows rather strong cross–isopycnal flow in the interior channel. Consequently, the diapycnal diffusivity K in TEM-G is rather large: Fig. 2 (d) shows the diagnosed eddy–induced diapycnal diffusivity (K) in TEM-G for experiment CHANNEL-3, with values of more than $100\,cm^2/s$ at maximum in the interior of the channel. Note that K inside the restoring zones is greatly exceeding $100\,cm^2/s$ and that K in TEM-G becomes negative in some interior regions near the restoring zones.

Going to higher resolution (and therefore less spurious diabatic forcing Q) changes the results only slightly. Fig. 3 a) and Fig. 4 a) show the residual streamfunction in TEM-G in experiments CHANNEL-6 and CHANNEL-12 respectively and Fig. 3 d) and Fig. 4 d) the respective eddy–induced diffusivities K in TEM-G. There is still strong cross–isopycnal flow in the residual streamfunctions and considerable large values of K in the higher resolution model configurations. Note that the regions in which K in TEM-G is negative remain more or less the same in all experiments and, if anything, show evidence of expanding into the interior.

In TEM-G, the eddy–induced diapycnal diffusivity K vanishes only if the eddy tracer fluxes are directed entirely along isopycnals. It is however unclear if the fluxes will locally satisfy $\mathbf{F} \cdot \nabla \bar{b} = 0$ in the adiabatic limit when $Q = 0$, i. e. it is unclear if statement i) is satisfied by TEM-G. Using the TEM-G flux decomposition in the integral constraint Eq. (5)

$$\int_{s_0}^{s_1} \overline{\mathbf{u}'b'} \cdot \mathbf{n}\, ds = -\int_{s_0}^{s_1} K|\nabla \bar{b}| ds = \int_A dA(\bar{Q} - \frac{\partial}{\partial t}\bar{b}) \tag{13}$$

it becomes clear that only a "mean" K in TEM-G averaged along a mean isopycnal (and weighted by $|\nabla \bar{b}|$) becomes zero in the adiabatic and quasi–steady case, while this cannot be

shown for the local value of K. In our numerical experiments, which are in quasi–steady state, K in TEM-G is large and fluctuates around zero on a mean isopycnal and this behavior does not decrease going to less diabatic flow regimes in higher resolution. Thus, on the basis of our numerical experiments in which we have done our best to come close to the adiabatic case, we conclude that TEM-G is not in accordance with statement i).

Finally, we discuss the boundary conditions related to TEM-G. Because the instantaneous flow and also the mean and eddy flow has zero normal velocity at boundaries we find that $\mathbf{F}\cdot\mathbf{a} = 0$ at the boundaries must hold, where $\mathbf{a}$ denotes a vector perpendicular to the boundaries. It would be desirable if there is also no advective tracer flux in the flux decomposition Eq. (10) across the boundaries, i. e. $B = const$ along the boundaries, which implies $\mathbf{u}_{eddy} \cdot \mathbf{a} = 0$, to obtain a consistent flux decomposition. On the boundary the tracer eddy flux is given by $\mathbf{F} = F_b \underset{\neg}{\mathbf{a}}$ where F_b is the component parallel to the boundary, hence $B = |\nabla\bar{b}|^{-1} F_b \ \mathbf{a} \cdot \nabla\bar{b}$. Consequently, we can get $B = 0$ on solid boundaries if $\mathbf{a} \cdot \nabla\bar{b} = 0$. This is the no-flux condition if Q is specified as harmonic (sub–grid–scale) mixing, i.e. $Q = \nabla \cdot (K_{sub} \nabla b)$ for some mixing coefficient K_{sub}. In our numerical model, the sub–grid–scale diffusive flux (given by the implicit diffusion in the Quicker advection scheme) associated with Q is set to zero at the boundaries, regardless of the normal gradient of b to the boundary, which implies that $\nabla\bar{b}$ is not normal to $\mathbf{a}$. Consequently, B in TEM-G is not zero at the boundaries in the numerical experiments, as seen in the figures.

However, the case that $\underset{\neg}{\nabla\bar{b}}$ parallels $\mathbf{a}$ yields $B = 0$ at the boundaries in TEM-G, a case which is implied by specifying Q as harmonic mixing. On the other hand, different specifications of Q, such as biharmonic mixing or Newtonian damping, do not necessarily constrain the normal gradient of b to the boundaries such that $\mathbf{a}$ parallels $\underset{\neg}{\nabla\bar{b}}$. For these specifications, B in TEM-G will be in general non–zero at the boundaries and there will be an advective eddy tracer flux through the boundaries, which is balanced by a diffusive flux related to K. Note that even for adiabatic and quasi–steady flows, B in TEM-G might still be non–vanishing at the boundaries since K will vanish only in an integral sense. As a solution for the boundary value problem for B it is sometimes proposed to change the flux decomposition of $\mathbf{F}$ near the boundaries to components parallel and perpendicular to the boundaries (Killworth, 2001; Held and Schneider, 1999) or by introducing additional boundary layers to absorb the advective flux through the boundary and in which B goes to zero (Killworth, 2001).

4 The adiabatic Transformed Eulerian Mean (TEM-A)

In TEM-G, the eddy–induced diapycnal diffusivity K vanishes only if the eddy tracer fluxes are entirely along isopycnals. It is however unclear if the fluxes will locally satisfy $\mathbf{F} \cdot \nabla \bar{b} = 0$ in the adiabatic limit when $Q = 0$, i. e. statement i) is not likely satisfied by TEM-G. In fact, the numerical experiments discussed above show that K in TEM-G is large for weakly diabatic flow, does not reduce much reducing Q, and furthermore fluctuates around zero along a mean isopycnal.

For this reason, we try to minimize the remainder (δ, η or K) which is due to the non–advective character of the eddy tracer fluxes in the mean tracer budget. First, we obtain a solution with zero K for the adiabatic case in this section, followed by a formal minimization for the diabatic case in the next section. Consider the flux decomposition

$$\mathbf{F} \;=\; \underset{\neg}{\nabla}\theta + B\, \underset{\neg}{\nabla}\bar{b} - K\nabla\bar{b} \tag{14}$$

where $\underset{\neg}{\nabla}\theta$ serves as a rotational gauge flux which drops out from the divergence of $\mathbf{F}$. Note that Eq. (14) is not a classical Helmholtz decomposition, since we are not insisting that all of the rotational part of the eddy tracer flux $\mathbf{F}$ is carried by $\underset{\neg}{\nabla}\theta$. The remainder $\mathbf{F} - \underset{\neg}{\nabla}\theta$ might still show some rotational part. The eddy streamfunction B and diapycnal diffusivity K are now given by

$$B \;=\; |\nabla\bar{b}|^{-2}(\mathbf{F} - \underset{\neg}{\nabla}\theta)\cdot \underset{\neg}{\nabla}\bar{b} \quad , \quad K = -|\nabla\bar{b}|^{-2}(\mathbf{F} - \underset{\neg}{\nabla}\theta)\cdot\nabla\bar{b} \tag{15}$$

It is useful to rewrite Eq. (15) as

$$B \;=\; |\nabla\bar{b}|^{-1}(F_{||} - \frac{\partial}{\partial n}\theta) \quad , \quad K = -|\nabla\bar{b}|^{-1}(F_{\perp} + \frac{\partial}{\partial s}\theta) \tag{16}$$

in terms of the along ($F_{||}$) and cross ($F_{\perp}$) isopycnal components of the eddy tracer flux and the along, $\frac{\partial}{\partial s}() = \mathbf{s}\cdot\nabla()$, and cross, $\frac{\partial}{\partial n}() = \mathbf{n}\cdot\nabla()$, isopycnal derivatives.

Since $\underset{\neg}{\nabla}\theta$ makes no contribution to the mean tracer budget, we have flexibility in the choice of θ, a flexibility we now exploit. Setting

$$\theta = -\int_{s_0}^{s} F_{\perp}\, ds' \tag{17}$$

we get obviously zero eddy–induced diapycnal diffusivity

$$K = -|\nabla\bar{b}|^{-1}(F_{\perp} + \frac{\partial\theta}{\partial s}) = 0 \tag{18}$$

For quasi–steady and adiabatic flow, the integral constraint Eq. (5) shows that θ will integrate to zero from one lateral boundary to the other lateral boundary in, e. g. the channel shown in Fig. 2 a). Since the integral constraint must hold for any mean isopycnal we obtain as boundary conditions $\theta = const$ along the boundaries. Therefore, there is no flux carried by $\underset{\neg}{\nabla}\theta$ across the boundaries. Since $K = 0$, all the eddy tracer flux must be carried by $B\ \underset{\neg}{\nabla}\bar{b}$ across the boundary and for arbitrary $\underset{\neg}{\nabla}\bar{b}$ at the boundary the eddy streamfunction B must be zero along the boundary, which gives a well–defined setting. Note that this is not true for TEM-G for quasi–steady and adiabatic flow.

Using this eddy tracer flux decomposition in the mean tracer budget with $Q = 0$ yields

$$\bar{b}_t + (\bar{\mathbf{u}} - \underset{\neg}{\nabla} B) \cdot \nabla \bar{b} \ = \ 0 \tag{19}$$

For $\bar{b}_t = 0$, the residual flow is purely along contours of $\bar{b}$ and only a non–zero $\bar{b}_t$ can force cross–isopycnal residual flow. We stress that these features are the essentials of what we know from the layered framework; that is, in agreement with statement i) from section 1. We call this flux decomposition for the adiabatic and quasi–steady case the adiabatic TEM, thus TEM-A.

Using the flux decomposition Eq. (14) and the definition Eq. (17) for θ, i. e. applying TEM-A, to diabatic flows is of course mathematically possible[6] in the general case, but yields an inconsistency. This can be seen considering again the integral constraint Eq. (5) for diabatic flows and using the definition Eq. (17) for θ

$$\theta|_{s_1} - \theta|_{s_0} = \int_{s_0}^{s_1} F_\perp ds = \int_A dA(\bar{Q} - \frac{\partial}{\partial t}\bar{b}) \tag{20}$$

This shows that starting the integration of θ at one lateral boundary at $s = s_0$ where the mean isopycnal intersects, must yield a different value of θ at the other boundary at $s = s_1$, since the cross–isopycnal eddy flux does not integrate to zero. Since θ acts as a streamfunction for a rotational eddy flux, there must be a rotational eddy flux through the lateral boundary at s_1 given by $\int_A dA(\bar{Q} - \frac{\partial}{\partial t}\bar{b})$. Thus setting $K = 0$ by the choice of θ in TEM-A for diabatic flows redirects the integrated cross–isopycnal eddy flux as a rotational flux through the boundary, a rather unphysical result. Note also that B will be not zero at the boundaries if TEM-A is applied to the diabatic case, since the cross–boundary rotational flux must be balanced by an advective flux.

[6] In the case of a closed contour of $\bar{b}$ this is not possible. Instead we get $K = -|\nabla\bar{b}|^{-1} \oint F_\perp ds$, see below. The minimal diffusivity K in the case of closed contours of $\bar{b}$ is given by the averaged and weighted eddy tracer flux across the respective closed contour of $\bar{b}$. However, note that this case cannot apply in the case of isopycnal coordinates for which closed isopycnals are not permitted.

However, even though applying TEM-A to diabatic flows yields an inconsistency, it is useful as a diagnostic tool to deduce the mean diabatic forcing $\bar{Q}$ in the numerical experiments. Note that estimating the "real" diabatic forcing in numerical models is rather difficult (Griffies et al., 2000; Eden and Oschlies, 2005), since there are no numerical advection schemes (even without any implicit diffusion, such as the classical "leapfrog"–scheme) which show the same properties as analytical advection, with the consequence that errors in the schemes have to be interpreted as diabatic forcing. Applying TEM-A in the diabatic case yields

$$\bar{b}_t + (\bar{\mathbf{u}} - \underset{\neg}{\nabla} B) \cdot \nabla \bar{b} \;=\; \bar{Q} \tag{21}$$

i. e. only a nonzero $\bar{Q}$ can force diapycnal residual flow in the quasi–steady budget for $\bar{b}$. To diagnose TEM-A in the numerical experiments, θ is calculated by interpolating $\mathbf{F}(y, \bar{b}(y,z)) \cdot \nabla\bar{b}/|\nabla\bar{b}|$ to an equidistant grid in the new coordinate $\bar{b}$ and integrating this quantity along lines of constant $\bar{b}$, starting at the southern end of the channel, where we put $\theta = 0$. In this way, we obtain $\theta(y,\bar{b}) = -\int_{s_0}^{s} F_\perp ds'$ and then interpolate θ back to z as vertical coordinate. This θ serves than as the boundary condition to solve the Euler–Lagrange Eq. (23). Note that the last step is formally not needed, but smoothes the solution for θ.

Fig. 2 (b) shows the (residual) streamfunction for the total (meridional) flow $(\bar{\mathbf{u}} - \underset{\neg}{\nabla} B)$ for TEM-A in experiment CHANNEL-3. In contrast to TEM-G (Fig. 2 a), the residual flow of TEM-A in the interior of the channel is more or less aligned along isopycnals with very little flow across isopycnals. Only inside the restoring zones the residual streamfunction in TEM-A shows large cross–isopycnal flow. The eddy–induced diapycnal diffusivity K in TEM-A (Fig. 2 e) fluctuates around zero diapycnal diffusivity, as expected by construction[7]. In TEM-A any cross–isopycnal (quasi–steady) flow is entirely driven by $\bar{Q}$. Therefore, we can conclude that the term $\nabla \cdot K\nabla\bar{b}$ in TEM-G drives the strong cross–isopycnal residual flow in the interior channel compared to TEM-A. K in TRM-G must be therefore much larger than an equivalent (mean) diapycnal diffusivity in $\bar{Q}$. Evaluating $\bar{Q}$ as the residual of $(\bar{\mathbf{u}} - \underset{\neg}{\nabla} B) \cdot \nabla\bar{b}$ in TEM-A (with $G(n) = 0$) in the interior channel model shows that $\bar{Q}$ is indeed an order of magnitude smaller than $\nabla \cdot K\nabla\bar{b}$ in TEM-G (not shown).

Going to higher resolutions in CHANNEL-6 and CHANNEL-12, the picture in TEM-A hardly changes, the residual streamfunction is aligned along mean isopycnals in the interior of the channel, indicating that $\bar{Q}$ might not change much in the higher resolution models. Fig. 5

[7] Inside the restoring zones near the side walls of the channel, however, larger residuals of K in TEM-A show up for numerical reasons. Note that this artifact vanishes going to higher resolution, as in experiment CHANNEL-6 and CHANNEL-12, discussed below. Note that for TEM-D (see below) the same artifact shows up in CHANNEL-3 and vanishes as well in CHANNEL-6 and CHANNEL-12.

(a,c,e) shows θ for the different experiments. Note that θ acts as a streamfunction for the rotational eddy tracer flux. As expected, there is a strong rotational eddy flux through the surface and the northern lateral boundary in all experiments, showing the strong diapycnal eddy fluxes. This rotational eddy flux through the boundaries is reduced in the higher resolution experiments, showing that the diapycnal eddy flux integrated along a mean isopycnal has decreased by lowering the instantaneous diabatic forcing Q, which means in turn that the diabatic forcing $\bar{Q}$ above the mean isopycnals has also decreased.

5 The diabatic Transformed Eulerian Mean (TEM-D)

TEM-A yields zero eddy–induced diffusivity K and consistent boundary conditions for adiabatic flows. For diabatic flows, however, TEM-A yields an inconsistent rotational eddy tracer flux through the boundaries. On the other hand, TEM-G shows large rotational eddy tracer fluxes in the interior leading to large K of fluctuating sign, as shown in the above section. We proceed to ask for a θ in the flux decomposition in Eq. (14) that minimizes (in some sense) $K\nabla\bar{b}$ (that is the cross–isopycnal eddy flux, when specifying b as potential density) but does not show the inconsistency in TEM-A. This leads to the following minimization problem

$$\frac{1}{2}\int W(K\nabla\bar{b})^2 dydz = min \tag{22}$$

where $W(y,z)$ denotes a weighting function which is specified below. The corresponding Euler–Lagrange equation[8] is

$$\underset{\neg}{\nabla}\bar{b}\cdot\nabla\left[\frac{W}{|\nabla\bar{b}|^2}\left(\mathbf{F}\cdot\nabla\bar{b}+\nabla\theta\cdot\ \underset{\neg}{\nabla}\bar{b}\right)\right]=0 \tag{23}$$

which states that the term inside the brackets is constant along contours of $\bar{b}$. It is convenient to use again coordinates along (s) and perpendicular (n) to contours of $\bar{b}$ for the bracketed term so that

$$F_\perp(s,n)+\frac{\partial\theta(s,n)}{\partial s}=G(n) \tag{24}$$

by specifying W as $W=|\nabla\bar{b}|$. We get as the optimal vector gauge potential

$$\theta(s,n)=\int_{s_0}^{s}(G(n)-F_\perp)ds'+H(n) \tag{25}$$

[8]Note that all results presented here carry over to three dimensions, including the solution of the Euler–Lagrange equation.

and for the eddy–induced diapycnal diffusivity, in turn,

$$K = -|\nabla\bar{b}|^{-1}(F_\perp + \frac{\partial\theta}{\partial s}) = -|\nabla\bar{b}|^{-1}G(n) \tag{26}$$

with arbitrary function $G(n)$ and $H(n)$. Note that a similar form of an optimal vector gauge θ and in turn an optimal streamfunction B was also mentioned in passing in Gille and Davis (1999). Setting the integration constant $G(n)$ to zero, we get zero eddy–induced diffusivity K as the minimal value, i. e. TEM-A is recovered. However, to obtain no rotational eddy tracer flux through the boundaries in the diabatic case, we must insure that $\theta = const$ along the boundaries, i. e.

$$G(n) = (s_1 - s_0)^{-1} \int_{s_0}^{s_1} F_\perp(s,n)ds = F_{ave}(n) \tag{27}$$

For this choice there is an eddy–induced diffusivity given by the diapycnal eddy fluxes averaged along an isopycnal. The difference to TEM-G is that it is not the local diapycnal eddy flux which determines K but the averaged flux. What is left in K is the minimal diapycnal flux which is needed to constrain the no-flow boundary condition for the rotational eddy flux. We call this flux decomposition TEM-D. Note that $K|\nabla\bar{b}|$ averaged along an isopycnal in TEM-D is the same as $K|\nabla\bar{b}|$ averaged along an isopycnal in TEM-G, But because TEM-G is not a solution of the minimization given by Eq. (23) the integral Eq. (22) evaluated for K in TEM-G must be larger than the integral for K in TEM-D.

TEM-D approaches TEM-G in the following limit: If the eddy tracer flux is entirely along contours of $\bar{b}$, i. e. if $\mathbf{F} \cdot \nabla\bar{b} = 0$ everywhere, the rotational potential θ and in consequence the rotational eddy tracer flux is zero. For this case the eddy streamfunction and diffusivity (which is also zero) become the same as in the TEM-G, and in the limits $|\bar{b}_z| << |\bar{b}_y|$ or $|\bar{b}_z| >> |\bar{b}_y|$ the same as in the TEM-II and TEM-I, respectively. Approaching the adiabatic limit, $Q = 0$, TEM-D becomes TEM-A under general circumstances. Note that TEM-G does not necessarily approach TEM-A in this limit. Therefore, TEM-D is in accordance with statement i) while TEM-G disagrees with it.

As in TEM-G, there will be an advective tracer flux associated with the eddy streamfunction B across the boundaries in TEM-D balanced by a diffusive flux associated with K, as long as $\mathbf{a}$ (the vector perpendicular to the boundaries) is not parallel to $\nabla\bar{b}$. It is only in the adiabatic, quasi–steady state, in which TEM-D becomes TEM-A, that B becomes zero at the boundaries. In diabatic flows this is obviously not possible while still satisfying the minimal constraint Eq. (23) at the same time.

In order to diagnose TEM-D in the numerical experiments, we simply use $\theta = 0$ as boundary condition to solve Eq. (23). Fig. 2 (c) shows the (residual) streamfunction for the total (meridional) flow ($\bar{\mathbf{u}} - \underline{\nabla} B$) in TEM-D in experiment CHANNEL-3. The cross–isopycnal residual flow ranges in between the strong cross–isopycnal flow in TEM-G (Fig. 2 a) and the almost vanishing cross–isopycnal flow in TEM-A (Fig. 2 b). Fig. 2 (f) shows the diagnosed eddy–induced diapycnal diffusivity K in TEM-D for experiment CHANNEL-3. It ranges in between the extreme cases TEM-G and TEM-A as expected from the cross–isopycnal flow of the residual streamfunctions. Note that while K in TEM-G becomes negative in some regions, this is not the case for TEM-D. Since $|\nabla \bar{b}|$ does not vary much in our numerical experiments, K in TEM-D shows almost no structure along a mean isopycnal. These uniform values of K reduce from about $100\,cm^2/s$ in CHANNEL-3 to about $50\,cm^2/s$ in CHANNEL-6 and about $20\,cm^2/s$ in CHANNEL-12. In all experiments, K in TEM-D is essentially an average over the very large K's of TEM-G inside the restoring zone near the side walls of the channel and the lower values in the interior.

Fig. 5 (b,d,f) shows θ in TEM-D for experiment CHANNEL-3, CHANNEL-6 and CHANNEL-12, respectively. It is clear that rotational cross–boundary fluxes are zero in this flux decomposition. However, there are strong rotational fluxes in the interior in all experiments. Note that the vertical rotational fluxes ($-\frac{\partial}{\partial y}\theta$) are of the same magnitude as the advective fluxes ($-B\frac{\partial}{\partial y}\bar{b}$) and the diffusive fluxes ($-K\frac{\partial}{\partial z}\bar{b}$) in all experiments and that the meridional rotational fluxes ($\frac{\partial}{\partial z}\theta$) are of the same magnitude as the advective fluxes ($B\frac{\partial}{\partial z}\bar{b}$) while the meridional diffusive fluxes are orders of magnitude smaller. This demonstrates again the importance of the rotational fluxes in setting the shape and magnitudes of the eddy streamfunction B and the diffusivity K. Note also that the interior rotational fluxes become stronger in magnitude going to higher resolution, rather than getting smaller.

Both TEM-D and TEM-A are consistent with statement i) and therefore they are consistent flux decompositions, and both involve a nonlocal definition of the rotational gauge potential θ. In TEM-D, this non–locality leads to an eddy–induced diffusivity which contains information throughout the channel about the strong diabatic forcing in the restoring zones near the northern and southern boundaries, even in regions in the interior which might be completely adiabatic. This is somehow an unsatisfactory result. In the next section, we will therefore try to find other flux decompositions, which will give a more local definition of θ and the eddy–induced diffusivity.

6 The (a)diabatic Temporal Residual Mean

Adding a rotational non–divergent part to the eddy tracer fluxes $\mathbf{F}$ does not effect the mean tracer budget. However, it does effect the eddy variance equation, offering an opportunity to interpret this part of the flux. This fact was used by McDougall and McIntosh (1996) to develop the Temporal Residual Mean (TRM-I hereafter) extension to the TEM theory and later the TRM–II version (McDougall and McIntosh, 2001). We discuss here the more general and – in this context – simpler derivation, similar to what can be found in Greatbatch (2001) and Medvedev and Greatbatch (2004), and compare it with the above presented TEM-A.

The eddy tracer fluxes are again expressed as in Eq. (14) where $\underline{\nabla}\theta$ serves as a gauge flux which drops out when taking the divergence of $\mathbf{F}$ and so does not contribute to the mean tracer budget. Motivation for choosing a non-zero rotational potential θ comes from the budget of tracer variance ($\overline{\phi}_2 = \overline{b'^2}/2$), given by

$$(\overline{\phi_2})_t + \nabla \cdot \overline{\mathbf{u}\phi_2} \;=\; \overline{b'Q'} - \underline{\nabla}\theta \cdot \nabla\bar{b} + K|\nabla\bar{b}|^2 \tag{28}$$

in which the decomposition (Eq. (14)) for $\mathbf{F}$ is used. We now decompose the total (i. e. mean plus eddy) flux of eddy tracer variance into components along and across contours of $\bar{b}$ plus a rotational part, as we did before for the eddy tracer flux $\mathbf{F}$,

$$\overline{\mathbf{u}\phi_2} = \underline{\nabla}\theta_2 + B_2\,\underline{\nabla}\bar{b} - K_2\nabla\bar{b} \tag{29}$$

where B_2 and K_2 are given by

$$B_2|\nabla\bar{b}| \;=\; \overline{\mathbf{u}\phi_2}\cdot\mathbf{s} - \frac{\partial}{\partial n}\theta_2 \quad , \quad K_2|\nabla\bar{b}| = -\overline{\mathbf{u}\phi_2}\cdot\mathbf{n} - \frac{\partial}{\partial s}\theta_2 \tag{30}$$

This yields the following set of equations

$$\bar{b}_t + (\bar{\mathbf{u}} - \underline{\nabla}B)\cdot\nabla\bar{b} \;=\; \bar{Q} + \nabla\cdot K\nabla\bar{b} \tag{31}$$

$$(\overline{\phi_2})_t + \underline{\nabla}(\theta - B_2)\cdot\nabla\bar{b} \;=\; \overline{b'Q'} + K|\nabla\bar{b}|^2 + \nabla\cdot K_2\nabla\bar{b} \tag{32}$$

Note that K_2 does not resemble a diffusivity, although we are using a similar symbol as for the eddy–induced diapycnal diffusivity K. Furthermore, B_2 also does not resemble a streamfunction for the eddy–driven transport velocity of eddy tracer variance. However, B_2 and K_2 are related to the along– and cross–isopycnal flux of variance in the same way as B and K are related to the along– and cross–isopycnal eddy tracer flux, respectively.

As before we utilize the gauge freedom, now for θ and θ_2, to rephrase Eq. (31) and Eq. (32). We apply first for the rotational eddy tracer flux the choice $\theta = B_2$, such that the rotational

gauge potential is related to the along–isopycnal flux of variance. We will show below that we follow with this choice the ideas of Marshall and Shutts (1981); McDougall and McIntosh (1996) and Medvedev and Greatbatch (2004). Second, we have to specify the rotational eddy variance flux given by $\underset{\neg}{\nabla}\theta_2$, which will have an effect on K_2 in Eq. (32) as we show also below. Analogous to the discussion for TEM-A and TEM-D, we define an "adiabatic" TRM version (TRM-A hereafter), in which we set

$$\text{TRM-A:} \quad \theta_2 = -\int_{s_0}^{s} \overline{\mathbf{u}\phi_2} \cdot \mathbf{n}\, ds \tag{33}$$

and get $K_2 = 0$ (which can readily be seen from Eq. (30)), and a "diabatic" TRM version (TRM-D hereafter), in which we set

$$\text{TRM-D:} \quad \theta_2 = \int_{s_0}^{s} (G_2(n) - \overline{\mathbf{u}\phi_2} \cdot \mathbf{n})\, ds \tag{34}$$

and get $K_2 = -|\nabla\bar{b}|^{-1} G_2(n)$ with $G_2 = (s_1 - s_0)^{-1} \int_{s_0}^{s_1} \overline{\mathbf{u}\phi_2} \cdot \nabla\bar{b}|\nabla\bar{b}|^{-1}\, ds$ (using the same reasoning as for the definition of TEM-D). In TRM-D, it is easy to see that θ_2 will integrate to zero at the boundaries, thus, there will be no rotational variance flux through the boundaries. On the other hand, there will be a rotational cross–boundary flux of variance in TRM-A as long as the integrated diapycnal flux of variance will not vanish, analogue to the discussion of TEM-A/D.

However, it is possible to show that this integrated flux of variance will go to zero in the quasi–steady and adiabatic limit. Adding the budgets of eddy tracer variance $\bar{\phi}_2$ and the mean tracer variance $\frac{\bar{b}^2}{2}$ and integrating again over an area above a mean isopycnal in the channel yields

$$\int_{s_0}^{s_1} \overline{\mathbf{u}\phi_2} \cdot \mathbf{n}\, ds + \bar{b} \int_{s_0}^{s_1} F_\perp\, ds = \int_A \overline{bQ}\, dA - \int_A \frac{\partial}{\partial t}(\bar{\phi}_t + \frac{\bar{b}^2}{2})\, dA \tag{35}$$

We know that the integrated cross–isopycnal eddy tracer flux $F_\perp$ vanishes in the quasi–steady and adiabatic limit, and find that the integrated cross–isopycnal flux of eddy variance must also vanish in this limit. Thus in the quasi–steady and adiabatic limit, TRM-A and TRM-D are the same, similar as before for TEM-A and TEM-D. Furthermore, in this limit $K_2 = 0$ and $K = 0$ and all four flux decompositions collapse into a single one in that limit. Thus, as for TEM-A and TEM-D, the new TRM versions are consistent with statement i).

As a result of these flux decompositions, we have the mean tracer budget as given by Eq. (31), in which an eddy–induced diffusivity K shows up. Using the eddy variance equation this K is given in TRM-A and TRM-D as

$$K|\nabla\bar{b}|^2 \quad = \quad -\overline{b'Q'} + (\overline{\phi_2})_t - \nabla \cdot K_2 \nabla\bar{b} \tag{36}$$

with $K_2 = 0$ for TRM-A and $K_2 = -|\nabla\bar{b}|^{-1}G_2(n)$ for TRM-D. For the quasi–steady and adiabatic limit $K = K_2 = 0$ in both versions.

As demonstrated in Appendix A, the difference between TRM-A/TRM-D and the TRM version of Medvedev and Greatbatch (2004) (TRM-M hereafter) is given by assuming that $\theta_2 = 0$ in TRM-M. It follows that in TRM-M, K_2 is related to the cross–isopycnal flux of eddy variance and contributes to K as in Eq. (36). Note that this diapycnal flux is not guaranteed to be zero locally for adiabatic and quasi–steady flow, as before for the diapycnal eddy tracer flux $F_\perp$ in TEM-G. The difference between TRM-M and TRM-I (McDougall and McIntosh, 1996) is given by assuming further that $|b_z| >> |b_y|$ and $\overline{\mathbf{u}'\phi_2} \approx 0$. Therefore, both TRM-M and TRM-I are not in accordance with statement i) (although one might argue that TRM-I is in accordance with i) to $o(\alpha^3)$). The TRM-A decomposition of fluxes was anticipated by Greatbatch (2001) where the normal flux of eddy variance was overlooked. The flux decomposition given by Marshall and Shutts (1981) is also a special case of the TRM-A in which it is assumed that $\theta_2 = K_2 = 0$; that is, that the entire flux of variance is along contours of $\bar{b}$.

We proceed now by diagnosing the different TRM versions which we have defined so far in this section using output from experiment CHANNEL-6. First we note that the residual streamfunctions (and consequently K) for TRM-I (McDougall and McIntosh, 1996) and TRM-II (McDougall and McIntosh, 2001) (which can be seen as special cases for $|b_y| << |b_z|$ and $\overline{v'\phi_2} \approx 0$ of TRM-M as outlined in Appendix A) are virtually the same as in TEM-G. This is because there is almost no mean advection of eddy variance in this experiments. In consequence, there is significant diapycnal flow in both TRM-I and TRM-II versions. Since TRM-II is constructed so as to mimic isopycnal averaging, the implied diapycnal diffusivity in this case indicates the error that arises because formulae in the TRM-II case are given only to quadratic order in perturbation amplitude, higher order terms being neglected.

Further, we note that the rotational potential θ for TRM-A (as given by Eq. (33), not shown) is rather similar to θ in TRM-D and also similar to TRM-M. Fig. 6 shows θ in TRM-D and TRM-M. Significant differences between both flux decompositions only show up near the boundaries. Consequently, the eddy-induced diapycnal diffusivity K and streamfunction B in TRM-A are only slightly changed compared to K and B in TRM-D and TRM-M. Fig. 7 b) shows K in TRM-M and Fig. 8 b) shows B in TRM-M. The difference in K between TRM-A and TRM-M is given by the effect of the cross–isopycnal eddy variance fluxes. It appears that this term is small compared to the term related to dissipation of eddy variance in the present setup. In the quasi–steady state, the eddy–induced diffusivity for TRM-A is given by $K = -(\nabla\bar{b})^{-2}\overline{Q'b'}$. It follows that in TRM-A the covariance between forcing and density

perturbations drives a large diapycnal diffusivity, orders of magnitude larger than the effect of the mean diabatic forcing $\bar{Q}$.

7 The generalized Temporal Residual Mean (TRM-G)

It is possible to extend the ideas of Greatbatch (2001) to the full hierarchy of moments which yields a generalized form of TRM along the ideas of Marshall and Shutts (1981); McDougall and McIntosh (1996) and Greatbatch (2001) (TRM-G hereafter) and which avoids any non–local definition of the rotational gauge potential θ. As before, for the eddy tracer flux $\mathbf{F}$ and the eddy tracer variance flux, a similar flux decomposition is also applied to fluxes of higher order variances $\overline{\phi_n} = \overline{\frac{b'^n}{n}}$

$$\overline{\mathbf{u}\phi_n} = \underline{\nabla}\theta_n + B_n \underline{\nabla}\bar{b} - K_n \nabla\bar{b} \tag{37}$$

which yields the following set of equations

$$\bar{b}_t + (\bar{\mathbf{u}} - \underline{\nabla} B) \cdot \nabla\bar{b} = \bar{Q} + \nabla \cdot K\nabla\bar{b} \tag{38}$$

$$(\overline{\phi_2})_t + \underline{\nabla}(\theta - B_2) \cdot \nabla\bar{b} = \overline{b'Q'} + K|\nabla\bar{b}|^2 + \nabla \cdot K_2\nabla\bar{b} \tag{39}$$

$$(\overline{\phi_{n+1}})_t + \underline{\nabla}(n\theta_n - B_{n+1}) \cdot \nabla\bar{b} = n\overline{\phi_n Q} - n\bar{\phi}_n\bar{b}_t + nK_n|\nabla\bar{b}|^2 + \nabla \cdot K_{n+1}\nabla\bar{b} \tag{40}$$

Note that Eq. (40) gives the budget for the higher order moments $\overline{\phi_{n+1}}$ using the flux decomposition Eq. (37), the other two budgets are simply a repetition from above. We extend the ideas of Greatbatch (2001) and set $\theta = B_2$ and $n\theta_n = B_{n+1}$ in the full hierarchy of equations which yields the following set of equations for the eddy streamfunction B, the eddy–induced diffusivity K and the rotational gauge potential θ in TRM-G

$$B|\nabla\bar{b}| = F_\parallel - \frac{\partial}{\partial m}J_2 + \frac{1}{2}(\frac{\partial}{\partial m})^2 J_3 - \frac{1}{3!}(\frac{\partial}{\partial m})^3 J_4 + ... \tag{41}$$

$$K|\nabla\bar{b}| = -F_\perp - \frac{\partial}{\partial s}\theta \tag{42}$$

$$\theta = J_2 - \frac{1}{2}\frac{\partial}{\partial m}J_3 + \frac{1}{3!}(\frac{\partial}{\partial m})^2 J_4 - ... \tag{43}$$

as given by the flux decomposition Eq. (14), Eq. (29) and Eq. (37) and with the along–isopycnal fluxes $J_n = \overline{\mathbf{u}\phi_n} \cdot \mathbf{s}$ and the operator $\frac{\partial}{\partial m}() = \mathbf{n} \cdot \nabla|\nabla\bar{b}|^{-1}()$. Using the variance budgets Eq. (40) we can express the eddy–induced diapycnal diffusivity in quasi–steady state also as

$$K|\nabla\bar{b}|^2 = -\overline{b'Q'} + \mathcal{D}(\overline{\phi_2 Q}) - \frac{1}{2}\mathcal{D}^2(\overline{\phi_3 Q}) + \frac{1}{3!}\mathcal{D}^3(\overline{\phi_4 Q}) + ... \tag{44}$$

with the operator $\mathcal{D}() = \nabla \cdot \nabla\bar{b}|\nabla\bar{b}|^{-2}()$. We see that K in TRM-G will be zero in the adiabatic and quasi–steady regime, and thus TRM-G is in accordance with statement i). As a result, we have constructed a fully consistent flux decomposition based on the ideas of Marshall and Shutts (1981); McDougall and McIntosh (1996) and Greatbatch (2001), which can be evaluated for any stratification and to any order and which gives a locally– defined eddy–induced diffusivity and eddy streamfunction. This is the main result of this paper.

Imposing the no normal gradient boundary condition for b (e. g. by specifying Q as harmonic diffusion), it is also easy to see from Eq. (41) that B and θ will be zero on the boundaries for the diabatic case, as before for TEM-D. If the normal gradient of b is non–zero at the boundaries, there will be an advective flux through the boundaries balanced by a diffusive flux and a rotational flux[9]. Since $K = 0$ in TRM-G for the adiabatic case because of Eq. (44), the rotational potential θ in TEM-A is in this limit identical to θ in Eq. (43). Thus, since K and θ are identical, B in TRM-G is also identical to B in TEM-A in this limit and must be zero at the boundaries (as argued previously for TEM-A). It is also easy to see that the definition for the streamfunction B in TRM-G is identical to TEM-G in the first term of the series in Eq. (41), to TRM-A and TRM-M in the first and second term. The same holds for K in Eq. (42).

Fig. 7 shows the eddy–induced diffusivity K in TRM-G, calculated in CHANNEL-6 with increasing orders in perturbation amplitude. For Fig. 7 a) K is evaluated to the first term in the series, i. e. $K|\nabla\bar{b}| = -F_\perp$ which is the same as K in TEM-G; Fig. 7 b) uses K to the second term, which is the same as K in TRM-M; c) is to the third term and d) to 4.th term. There is a large decrease in magnitude of K in the interior of the channel going from the first term (a, equivalent to TEM-G) to the second term (b, equivalent to TRM-M). However, there are still regions of negative K in TRM-M. These regions are further reduced and are subsequently vanish including also higher order terms in TRM-G. On the other hand, the corrections to K are decreasing in higher orders, showing the rapid convergence of TRM-G in our experimental setup.

Note that the diffusivity K evaluated to the second term (Fig. 7 b) appears to be a reasonable approximation to the full form (excluding the regions of negative K). Since this K is almost identical to TRM-A we conclude that $K = -(\nabla\bar{b})^{-2}\overline{Q'b'}$ is a reasonable expression for a local definition of K to be used in a parameterization. Note also that there are still very large values of K in TRM-G inside the restoring zones, much larger than the "mean" value of K in TEM-D.

[9] Note that the rotational flux through the boundaries in the diabatic case in TRM-G for general boundary conditions of b can always be eliminated, redefining θ in TRM-G by introducing a nonlocal component similar to TRM-D and TEM-D. However, our experiments show that this rotational cross–boundary flux in small, see below.

On the other hand, interior values of K are small in TRM-G (or TRM-A) in the range of about $20\,cm^2/s$, i. e. much smaller than the corresponding averaged values of K in TEM-D. Fig. 8 shows the residual streamfunction in TRM-G, calculated in CHANNEL-6 again with increasing orders in perturbation amplitude.

8 Summary and discussion

The different eddy tracer flux decompositions

We have presented and named several different versions of the TEM and TRM flux decompositions. These are summarized in Table 1. We have identified the TEM-I version of Andrews and McIntyre (1976) and TEM-II version of Held and Schneider (1999) as special cases of a generalized TEM version, called TEM-G (Andrews and McIntyre, 1978). In all these TEM versions, a term related to an apparent eddy–induced diapycnal diffusion shows up. It was our aim, formulated in statement i) in Section 1, to represent the effect of eddy fluxes as a purely isopycnal flux in the adiabatic and quasi–steady case. This is not guaranteed to be the case for TEM-G. Moreover, as shown in Section 3, the implied eddy-induced diapycnal diffusion can become large with large changes of sign on a mean isopycnal. The numerical experiments show that this behavior does not reduce going to higher resolution and thus less diabatic forcing. We have identified rotational eddy tracer fluxes as being responsible for this behavior.

It is possible to set this diffusive term to zero by introducing a non–locally defined gauge flux in the eddy tracer fluxes. We call this flux decomposition the adiabatic Transformed Eulerian Mean or TEM-A, which can be applied to adiabatic flows only and which is in agreement with statement i). The eddy streamfunction in TEM-A will be zero on the boundaries, but this need not be true for TEM-G in the adiabatic case. However, applying TEM-A to diabatic flows yields an unphysical cross–boundary rotational eddy tracer flux.

By formulating a minimal condition for the cross–isopycnal tracer flux (which is, however, much different to a classical Helmholtz decomposition) we extend the TEM-A to diabatic regimes. This extension is called TEM-D. Here, an eddy-induced diapycnal diffusion shows up again in the mean tracer budget, which vanishes only in the adiabatic regime. We use this result as an argument in favor of eddy–induced diapycnal mixing for diabatic flows. TEM-D collapses to TEM-A in the adiabatic, quasi–steady limit, thus TEM-D is in agreement with statement i).

We have shown that TEM-G yields larger diapycnal diffusivity than TEM-D, even in the adiabatic case, i. e. TEM-G is introducing artificially large diapycnal eddy–induced diffusivities. In general, as in TEM-G, an advective eddy–induced flux will be balanced by an diffusive flux at the boundaries in TEM-D. Only when specifying no–normal gradient boundary conditions for the tracer, as usually assumed specifying the diabatic forcing as sub–grid–scale harmonic mixing, the eddy streamfunction will be zero at the boundary for TEM-D. However, since TEM-D collapses to TEM-A in the adiabatic limit, the streamfunction will be zero in that case, while this is not true for TEM-G.

However, since the eddy–induced diffusivity in TEM-D is constant along a mean isopycnal and is given by an average of the eddy tracer flux across this mean isopycnal, it can include information from strong non-local diabatic forcing even in completely adiabatic regions. In our numerical channel experiments, the strong forcing inside the restoring zones gives rise to large diffusivities in the interior (note that they are positive definite in all experiments). This is a rather unsatisfactory result. Furthermore, such a non–local definition of the diffusivity and streamfunction might be difficult to parameterize.

All TEM versions consider the first order moments. In contrast, the TRM versions consider the eddy tracer variance equation to find gauge fluxes for the eddy tracer flux. We have defined a TRM version, called TRM-A, which contains only a single diffusivity K which is given by the (local) rate of change and dissipation of eddy variance (as anticipated by Greatbatch (2001), and for which the decomposition proposed by Marshall and Shutts (1981) is a special case) by introducing a non–local gauge flux in the tracer variance fluxes. The gauge flux of the eddy tracer flux in TRM-A is given by the along–isopycnal flux of variance corrected by the gauge flux of the variance fluxes. Setting the gauge flux of the variance fluxes to zero leads to TRM-M by Medvedev and Greatbatch (2004), for which the special case $|b_z| >> |b_y|$ and $\overline{v'\phi_2} \approx 0$ leads to TRM-I by McDougall and McIntosh (1996).

As before for TEM-A, the flux decomposition TRM-A is formally not applicable to diabatic flows, because of spurious cross–boundary rotational fluxes in the diabatic regime. However, the numerical experiments show that these cross–boundary fluxes are much smaller compared to TEM-A applied to diabatic flows. Based on TRM-A, we have formulated a TRM version for the diabatic case (TRM-D), for which it was shown that it collapses to TRM-A and to TEM-A in the quasi–steady adiabatic limit. Thus TRM-D satisfies statement i) while this is not true for TRM-M or TRM-I, since here the eddy–induced diapycnal diffusivity does not necessarily vanish in the quasi–steady, adiabatic limit[10].

[10]Note that McDougall and McIntosh (1996) show that the diffusivity should be zero to cubic order in

As a final result, we have generalized the concept and found TRM-G which collapses to TEM-A in the quasi–steady and adiabatic limit, but avoids any integral definitions of the rotational gauge fluxes. In contrast, the eddy streamfunction and the eddy–induced diffusivity in TRM-G are given by an infinite series involving eddy tracer moments, since the flux decomposition was derived from an infinite hierarchy of budgets for tracer moments. Truncating the infinite series for the eddy–induced streamfunction and diffusivity in TRM-G after the first term gives TRM-G and truncating after the second term gives TRM-M by Medvedev and Greatbatch (2004). This new concept can be evaluated for any stratification, in three–dimensions, to any order, and is in agreement with statement i).

Discussion

We found that there is eddy–induced diapycnal mixing, if there is any instantaneous diapycnal mixing. In fact, the integral constraint Eq. (4) shows that only the eddy tracer flux can transport information about diabatic forcing across mean isopycnals in the integral budget. This effect is rather strong in our numerical model and might be overestimated, but we think, that the traditional view that eddy are mixing completely adiabatically has to be revised, as proposed by Radko and Marshall (2004) and Tandon and Garrett (1996).

In the ocean, diapycnal diffusivity drives large–scale flow, i.e. the thermohaline overturning. Estimating $\bar{Q}$ (as usually done by direct turbulence measurements) might be insufficient to get the effective diapycnal diffusivity. In other words, the small diapycnal mixing as estimated so far from direct observations in the ocean, might be enhanced by eddy activity. Note that it is in principle possible to evaluate K from direct observations.

Although the focus of the present paper is on interpreting eddy fluxes, diagnosed from numerical models or observations, the consistent eddy flux decompositions might also prove useful for parameterizing the effect of eddies, in particular the eddy–induced diapycnal mixing, for implementation in non–eddy–resolving models. We found that TRM-A is a good approximation to TRM-G and implies a rather simple form of the eddy–induced diapycnal diffusivity given by local dissipation of eddy tracer variance.

perturbation amplitude, an approximation that does not hold up in the numerical experiments.

Acknowledgments

We want to thank J. Willebrand, A. Oschlies, A. Medvedev and S. Danilov for stimulating discussions. We also thank two anonymous reviewers and the editor for helpful comments. The model integrations have been performed on a NEC–SX5 at the computing center at the University Kiel, Germany. RJG also thanks NSERC and CFACS for financial support through an NSERC Research Grant at the Canadian CLIVAR Research Network.

Appendix A

In this appendix we show the relation of TRM-A as presented in this paper with the flux decompositions TRM-I (McDougall and McIntosh, 1996), TRM-II (McDougall and McIntosh, 2001) and TRM-M (Medvedev and Greatbatch, 2004). As discussed in section 6, the choice $\theta = B_2$ and θ_2 such that $K_2 = 0$ leads to the TRM-A set of equations

$$(\overline{\phi_2})_t = \overline{b'Q'} + K|\nabla\bar{b}|^2 \tag{45}$$

$$\bar{b}_t + (\bar{\mathbf{u}} - \underset{\neg}{\nabla} B) \cdot \nabla\bar{b} = \bar{Q} + \nabla \cdot K\nabla\bar{b} \tag{46}$$

Setting instead $\theta = B_2$ and $\theta_2 = 0$, i. e. omitting all non–local gauge fluxes, a term related to the cross-isopycnal flux of eddy variance shows up in the eddy variance equation:

$$(\overline{\phi_2})_t = \overline{b'Q'} + K|\nabla\bar{b}|^2 + \nabla \cdot K_2\nabla\bar{b} \tag{47}$$

$$\bar{b}_t + (\bar{\mathbf{u}} - \underset{\neg}{\nabla} B) \cdot \nabla\bar{b} = \bar{Q} + \nabla \cdot K\nabla\bar{b} \tag{48}$$

with

$$B = |\nabla\bar{b}|^{-2}(\mathbf{F} - \underset{\neg}{\nabla} B_2) \cdot \underset{\neg}{\nabla}\bar{b} \quad , \quad K = -|\nabla\bar{b}|^{-2}(\mathbf{F} - \underset{\neg}{\nabla} B_2) \cdot \nabla\bar{b} \tag{49}$$

$$B_2 = |\nabla\bar{b}|^{-2}\overline{\mathbf{u}\phi_2} \cdot \underset{\neg}{\nabla}\bar{b} \quad , \quad K_2 = -|\nabla\bar{b}|^{-2}\overline{\mathbf{u}\phi_2} \cdot \nabla\bar{b} \tag{50}$$

The latter choice leads to TRM-M and further leads to TRM-I, for which it is additionally assumed that $|\bar{b}_z| >> |\bar{b}_y|$. We find for the eddy streamfunction B for $\theta_2 = 0$, $\theta = B_2$ and $|\bar{b}_z| >> |\bar{b}_y|$

$$\theta = B_2 \approx -\overline{v\phi_2}/\bar{b}_z \quad \text{and} \quad B \approx -(\overline{v'b'} + \theta_z)/\bar{b}_z \tag{51}$$

which is the TRM-I streamfunction as given by McDougall and McIntosh (1996) (their Eq. 11) except that they neglected additionally the triple correlation in the eddy variance fluxes; that

is, they assumed $\overline{v\phi_2} \approx \bar{v}\bar{\phi}$. The diffusivity K in TRM-M is given by

$$K = -|\nabla\bar{b}|^{-2}(\overline{Q'b'} - (\overline{\phi_2})_t + \nabla \cdot K_2\nabla\bar{b}) \tag{52}$$

and its effect in the mean tracer equation for $\bar{b}_z >> \bar{b}_y$ is given by

$$\nabla \cdot K\nabla\bar{b} \approx -\left(\frac{\overline{b'Q'}}{\bar{b}_z}\right)_z + \left(\frac{(\overline{\phi_2})_t}{\bar{b}_z}\right)_z + \left(\frac{1}{\bar{b}_z}\left(\frac{\overline{\mathbf{u}\phi_2}\cdot\nabla\bar{b}}{\bar{b}_z}\right)_z\right)_z \tag{53}$$

which can be shown to be the same as $\bar{Q}^{\#} - T_z - \bar{Q}$ in Eq. 12 of McDougall and McIntosh (1996). However, here, we haven't neglected the triple correlation in the flux of variance. TRM-M resembles therefore a generalization of TRM-I to the general situation without assuming $|\bar{b}_z| >> |\bar{b}_y|$ and the triple correlation. Note that in TRM-A the last term related to the cross–isopycnal variance flux in the above equation does not show up, since $K_2 = 0$ by construction. Note also that in the steady adiabatic limit, this term does not zero out in general, giving rise for a non–zero K even in this limit.

TRM-II attempts to mimic isopycnal averaging by a truncated (vertical) Taylor expansions of b and $\mathbf{u}$ and leads to a very similar definition of the eddy streamfunction as in McDougall and McIntosh (1996)

$$B \approx -(\overline{v'b'} - \bar{v}_z(\bar{\phi}_2/\bar{b}_z))/\bar{b}_z \tag{54}$$

and is (consequently) in our numerical experiments very similar to the TRM-I version of McDougall and McIntosh (1996). Note, however that the mean variables $\bar{b}$ and $\bar{\mathbf{u}}$ have been redefined in TRM-II, in such a way as to absorb the cross isopycnal flux of variance (again only the mean flux) into the definition of the new variable, making it difficult to relate the TRM-II with a diffusivity K.

References

Andrews, D. G. and M. E. McIntyre, 1976: Planetary waves in horizontal and vertical shear: The generalized Eliassen–Palm relation and the zonal mean accelaration. *J. Atmos. Sci.*, **33**, 2031–2048.

Andrews, D. G. and M. E. McIntyre, 1978: Generalized Eliassen–Palm and Charney–Drazin theorems for waves on axisymmetric mean flows in compressible atmosphere. *J. Atmos. Sci.*, **35**, 175–185.

Eden, C. and A. Oschlies, 2005: Effective diffusivities in model of the North Atlantic. Part I: subtropical thermocline. *J. Phys. Oceanogr.*. Submitted.

Gent, P. R., J. Willebrand, T. J. McDougall, and J. C. McWilliams, 1995: Parameterizing eddy-induced tracer transports in ocean circulation models. *J. Phys. Oceanogr.*, **25**, 463–474.

Gille, S. T. and E. E. Davis, 1999: The influence of mesoscale eddies on coarsely resolved density: an examination of subgrid–scale parameterization. *J. Phys. Oceanogr.*, **29**, 1109–1123.

Greatbatch, R. J., 2001: A framework for mesoscale eddy parameterization based on density-weighted averaging at fixed height. *J. Phys. Oceanogr.*, **31**(9), 2797–2806.

Griffies, S. M., R. C. Pacanowski, and B. R. Hallberg, 2000: Spurious diapycnal mixing associated with advection in a z-coordinate ocean model. *Mon. Wea. Rev.*, **128**, 538–564.

Hasselmann, K., 1982: An ocean model for climate variability studies. *Prog. Oceanogr.*, **11**, 69–92.

Held, I. M. and T. Schneider, 1999: The surface branch of the zonally averaged mass transport circulation in the troposphere. *J. Atmos. Sci.*, **56**(11), 1688–1697.

Killworth, P. D., 2001: Boundary conditions on quasi-stokes velocities in parameterisations. *J. Phys. Oceanogr.*, **31**, 1132–1155.

Leonard, B. P., 1979: A stable and accurate convective modelling procedure based on quadratic upstream interpolation. *Computer Methods in Applied Mechanics and Engineering*, **19**, 59–98.

Marshall, J. and G. Shutts, 1981: A note on rotational and divergent eddy fluxes. *J. Phys. Oceanogr.*, **11**(12), 1677–1679.

McDougall, T. J., 1987: Neutral surfaces. *J. Phys. Oceanogr.*, **17**, 1950–1964.

McDougall, T. J. and P. C. McIntosh, 1996: The temporal–residual–mean velocity. Part I: Derivation and the scalar conservation equation. *J. Phys. Oceanogr.*, **26**, 2653–2665.

McDougall, T. J. and P. C. McIntosh, 2001: The temporal-residual-mean velocity. Part II: Isopycnal interpretation and the tracer and momentum equations. *J. Phys. Oceanogr.*, **31**(5), 1222–1246.

Medvedev, A. S. and R. J. Greatbatch, 2004: On advection and diffusion in the mesosphere and lower thermosphere: The role of rotational fluxes. *J. Geophys. Res.*, **109**(D07104, 10.1029/2003JD003931).

Nakamura, N., 2001: A new look at eddy diffusivity as a mixing diagnostic. *J. Atmos. Sci.*, **58**, 3695–3701.

Nurser, A. J. G. and M.-M. Lee, 2004: Isopycnal averaging at constant height: Part I: the formulation and a case study. *J. Phys. Oceanogr.*, **34**(12), 2721–2739.

Olbers, D. and M. Visbeck, 2005: A zonally averaged model of the meridional overturning in the Southern Ocean. *J. Phys. Oceanogr.*. In press.

Pacanowski, R. C., 1995: MOM 2 Documentation, User's Guide and Reference Manual. Technical report, GFDL Ocean Group, GFDL, Princeton, USA.

Plumb, R. A. and R. Ferrari, 2005: Transformed eulerian-mean theory. Part I: Nonquasigeostrophic theory for eddies on a zonal-mean flow. *J. Phys. Oceanogr.*, **35**(2), 165–174.

Radko, T. and J. Marshall, 2004: Eddy–induced diapycnal fluxes and their role in the maintenance of the thermocline. *J. Phys. Oceanogr.*, **34**, 372–383.

Tandon, A. and C. Garrett, 1996: On a recent parameterization of mesoscale eddies. *J. Phys. Oceanogr.*, **26**(3), 406–416.

Wüst, G., 1935: Schichtung und Zirkulation des Atlantischen Ozeans. Die Stratoshäre des Atlantischen Ozeans. *Wiss. Ergebn. Dt. Atlant. Exped. "Meteor" 1925–1927*, **6**, 109–288.

List of Tables

List of Figures

Acronym	Meaning	Assumption	diapycnal diffusivity
TEM-I	Transformed Eulerian Mean (Andrews and McIntyre, 1976)	$\bar{b}_z >> \bar{b}_y$	$\delta/\bar{b}_z$
TEM-II	Transformed Eulerian Mean (Held and Schneider, 1999)	$\bar{b}_y >> \bar{b}_z$	$\eta/\bar{b}_y$
TEM-G	generalized TEM (Andrews and McIntyre, 1978)	-	$K = -\lvert\nabla\bar{b}\rvert^{-2}\overline{\mathbf{u}'b'}\cdot\nabla\bar{b}$
TEM-A	TEM adiabatic	$\oint \overline{\mathbf{u}'b'}\cdot\nabla\bar{b}\,ds = 0$	$K = 0$
TEM-D	TEM diabatic	-	$K \sim -\oint \overline{\mathbf{u}'b'}\cdot\nabla\bar{b}\,ds$
TRM-I	Temporal Residual Mean (McDougall and McIntosh, 1996)	$\bar{b}_z >> \bar{b}_y$, $\overline{v'\phi_2} \approx 0$	$\delta/\bar{b}_z$
TRM-II	Temporal Residual Mean (McDougall and McIntosh, 2001)	$\bar{b}_z >> \bar{b}_y$, $\overline{v'\phi_2} \approx 0$	see appendix B
TRM-M	Temporal Residual Mean by Medvedev and Greatbatch (2004)	$\theta_2 = 0$	see appendix B
TRM-A	TRM adiabatic	$\oint \overline{\mathbf{u}\phi_2}\cdot\nabla\bar{b}\,ds = 0$	$K = -\lvert\nabla\bar{b}\rvert^{-2}[\overline{Q'b'} - (\overline{\phi_2})_t]$
TRM-D	TRM diabatic	-	$K = -\lvert\nabla\bar{b}\rvert^{-2}[\overline{Q'b'} - (\overline{\phi_2})_t + \nabla\cdot K_2\nabla\bar{b}]$
TRM-G	generalized TRM	-	$K = -\lvert\nabla\bar{b}\rvert^{-2}(\overline{Q'b'} - \mathcal{D}(\overline{\phi_2 Q}) + ...)$

Table 1: Summary of names and features of the eddy flux decompositions discussed in the text. Note that the definition for K differ for each version.

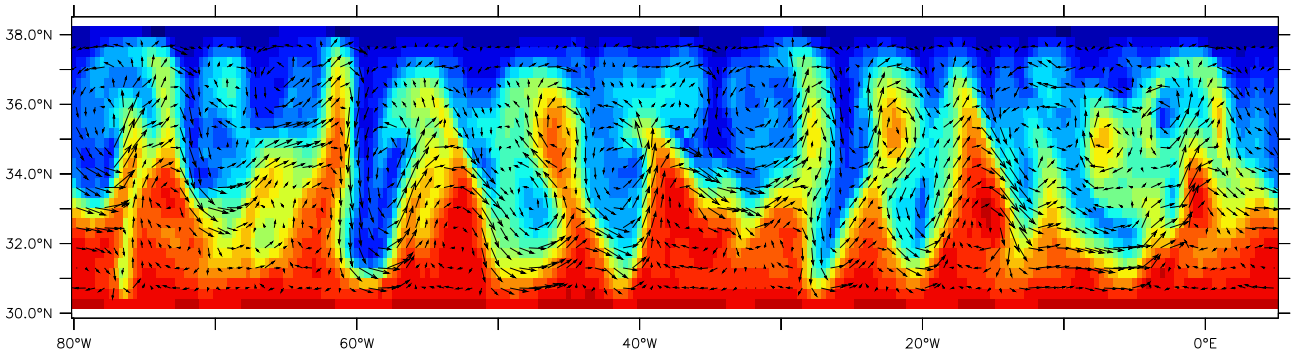

Figure 1: Instantaneous temperature and velocity at 1000m depth after one year integration in experiment CHANNEL-3. Every second velocity grid point is displayed and the color shading ranges from 2^oC to 12^oC

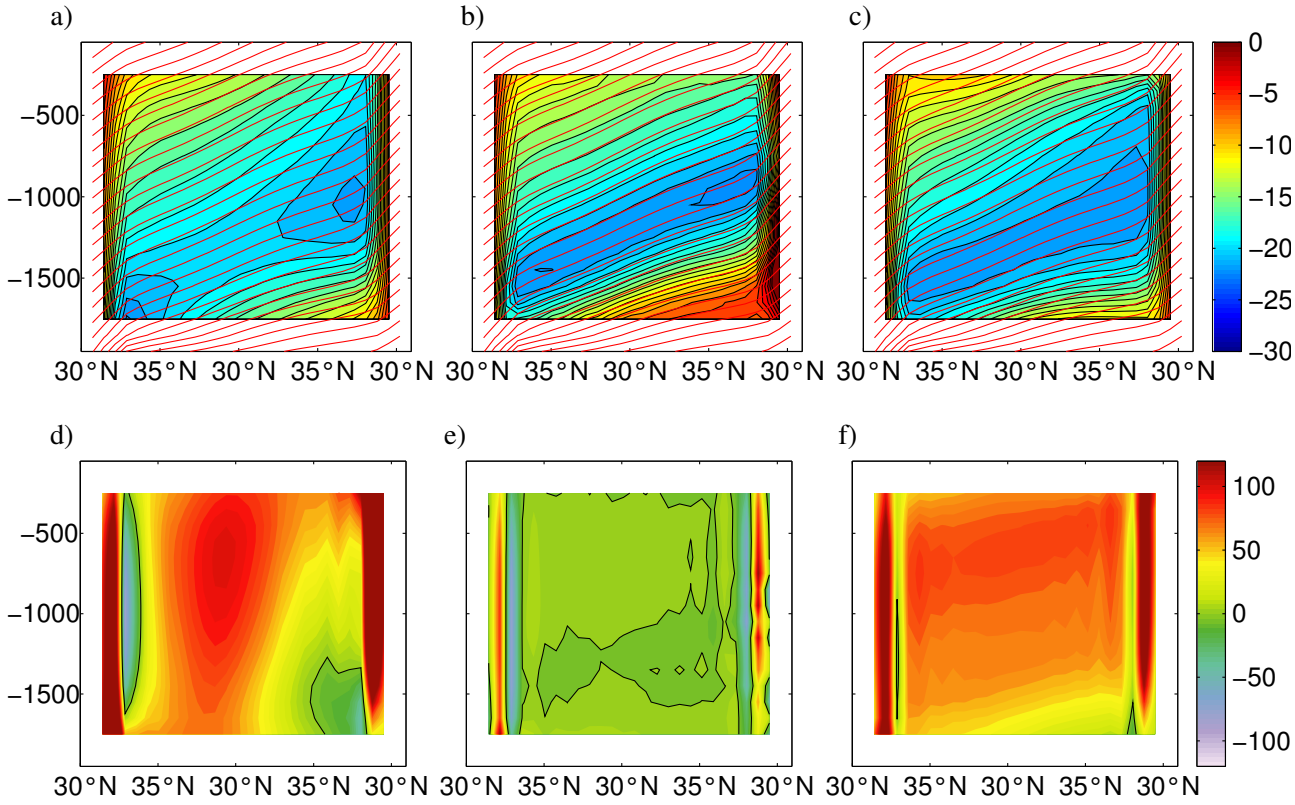

Figure 2: Upper row: Streamfunction for the total flow in TEM-G (a) in m^2/s, in TEM-A (b) and in TEM-D (c) in experiment CHANNEL-3. Contour interval is $1\,m^2/s$. Also shown are contours of $\bar{b}$ (red lines). Lower row: Eddy induced diffusivity K in cm^2/s in TEM-G (d), in TEM-A (e) and in TEM-D (f).

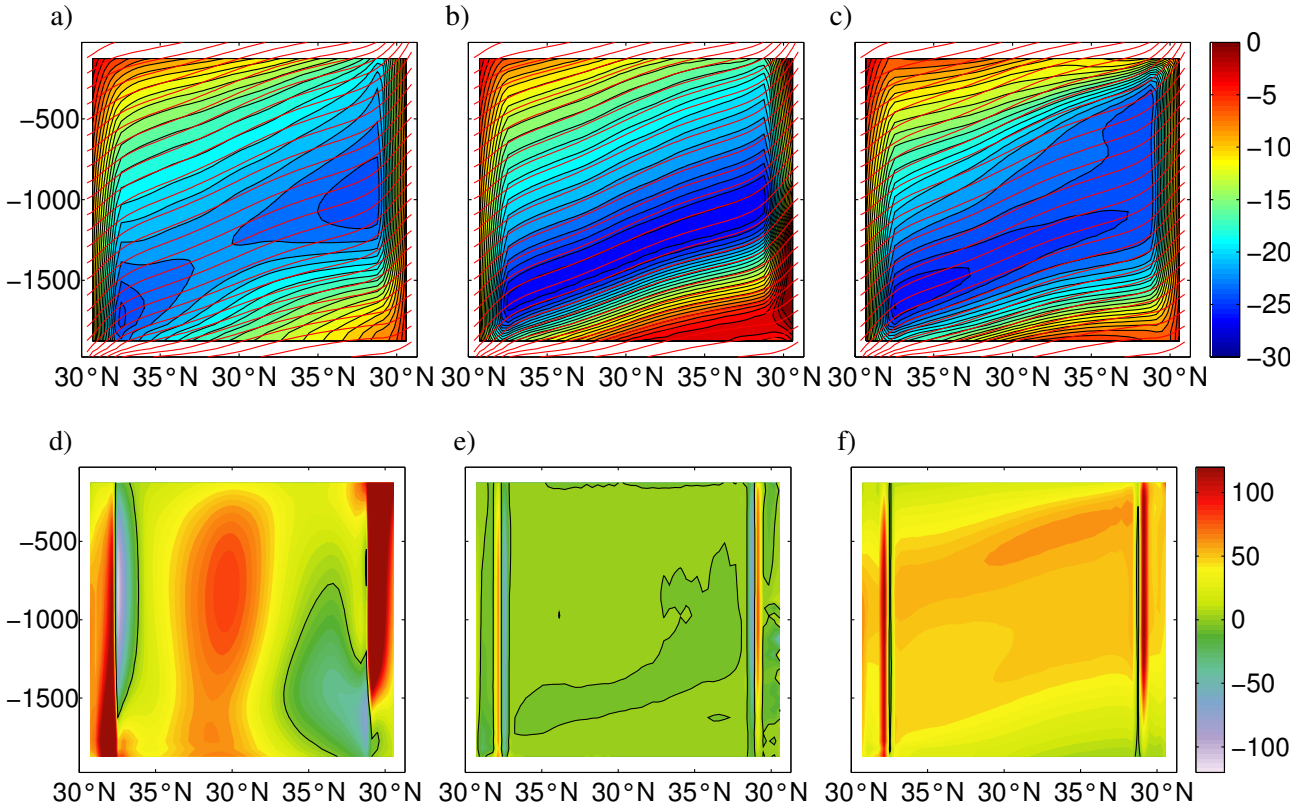

Figure 3: Upper row: Streamfunction for the total flow in TEM-G (a) in m^2/s, in TEM-A (b) and in TEM-D (c) in experiment CHANNEL-6. Contour interval is $1\,m^2/s$. Also shown are contours of $\bar{b}$ (red lines). Lower row: Eddy induced diffusivity K in cm^2/s in TEM-G (d), in TEM-A (e) and in TEM-D (f).

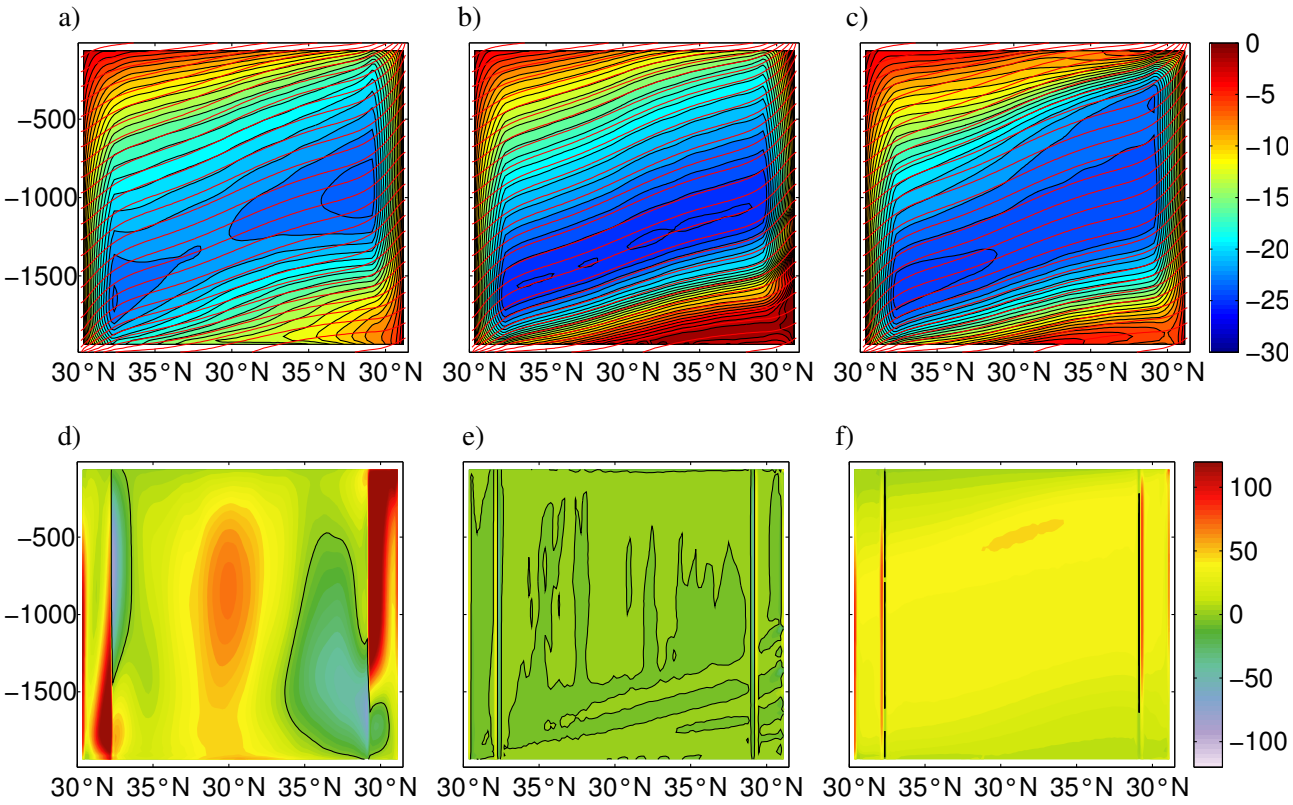

Figure 4: Upper row: Streamfunction for the total flow in TEM-G (a) in m^2/s, in TEM-A (b) and in TEM-D (c) in experiment CHANNEL-12. Contour interval is $1\,m^2/s$. Also shown are contours of $\bar{b}$ (red lines). Lower row: Eddy induced diffusivity K in cm^2/s in TEM-G (d), in TEM-A (e) and in TEM-D (f).

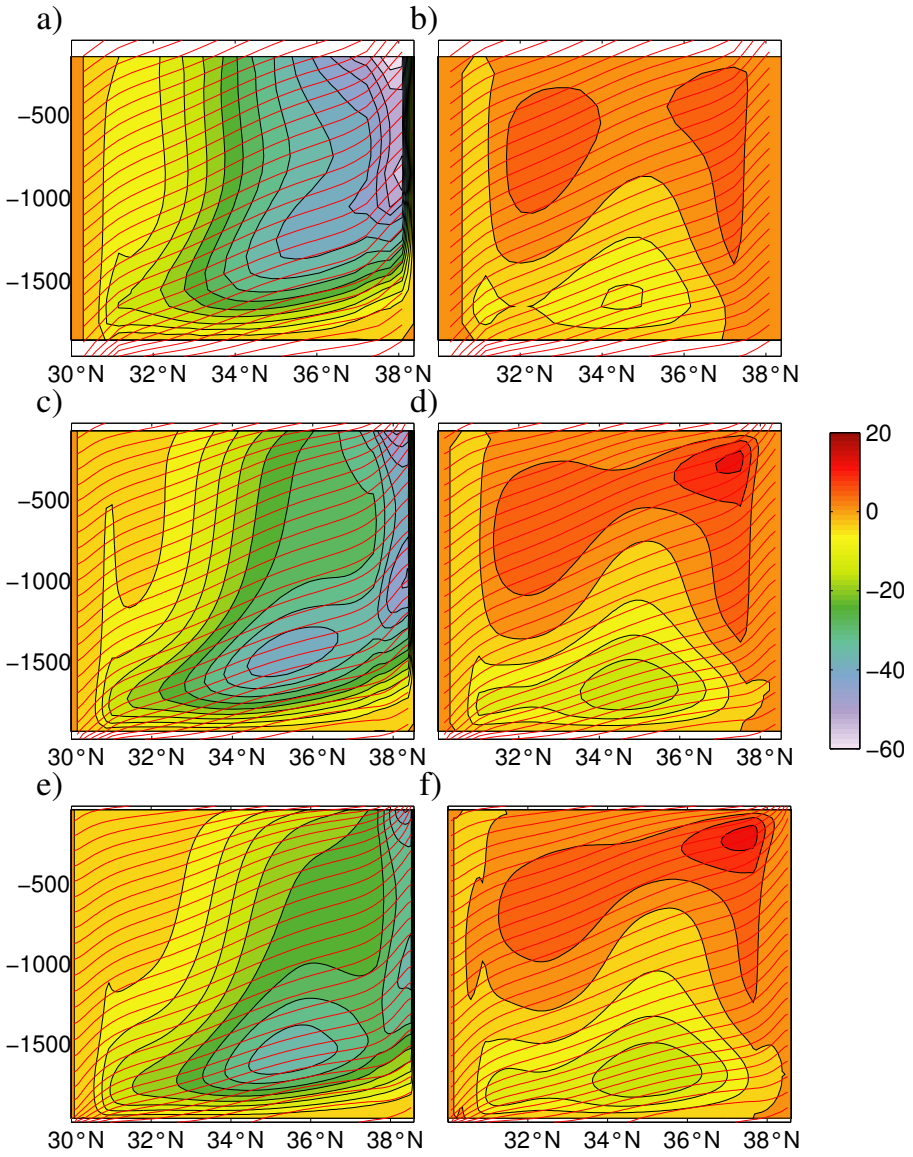

Figure 5: Rotational gauge potentials θ (in Km^2/s) in TEM-A (a,c,e) and TEM-D (b,d,f) in experiment CHANNEL-3 (a,b), CHANNEL-6 (c,d) and CHANNEL-12 (e,f).

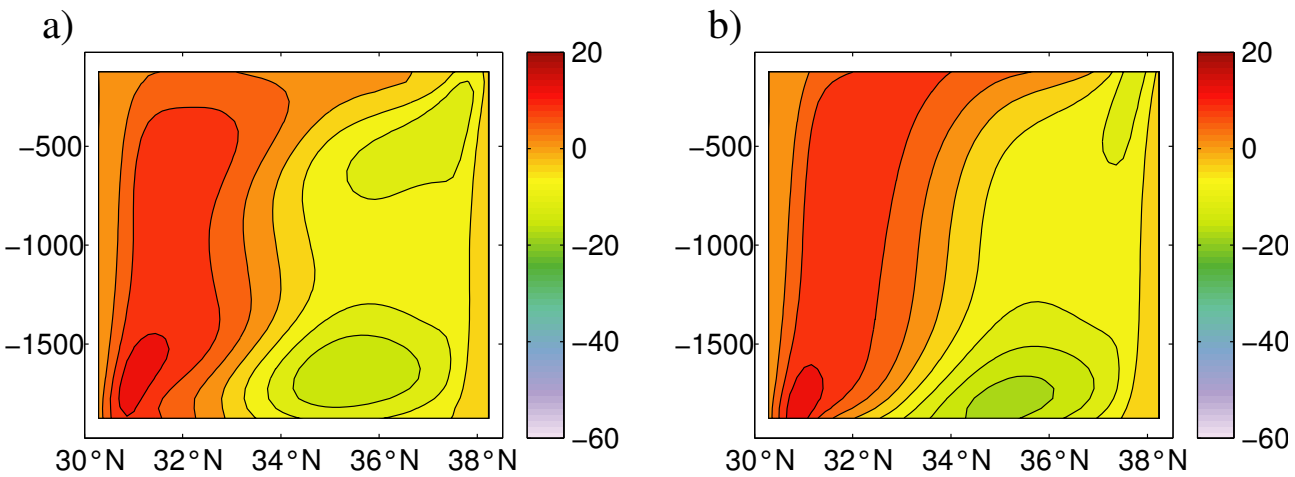

Figure 6: Rotational gauge potentials θ (in Km^2/s) in TRM-D (a) and TRM-M (b) in experiment CHANNEL-6.

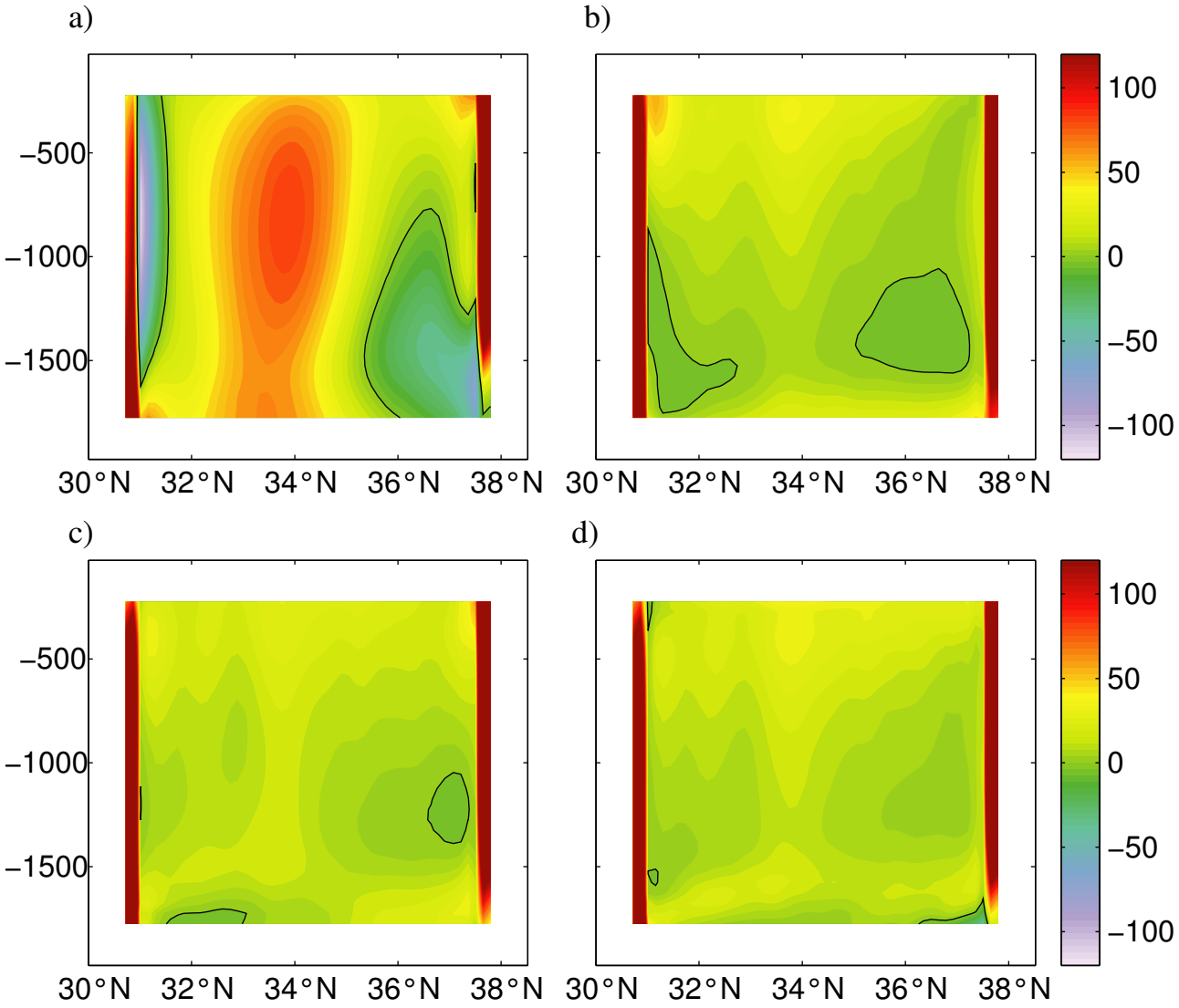

Figure 7: Eddy induced diffusivity K in cm^2/s in TRM-G calculated to first order (a), second order (b), third order (c) and 4.th order (d). Note that (a) is the same as K in TEM-G and (b) the same as K in TEM-M.

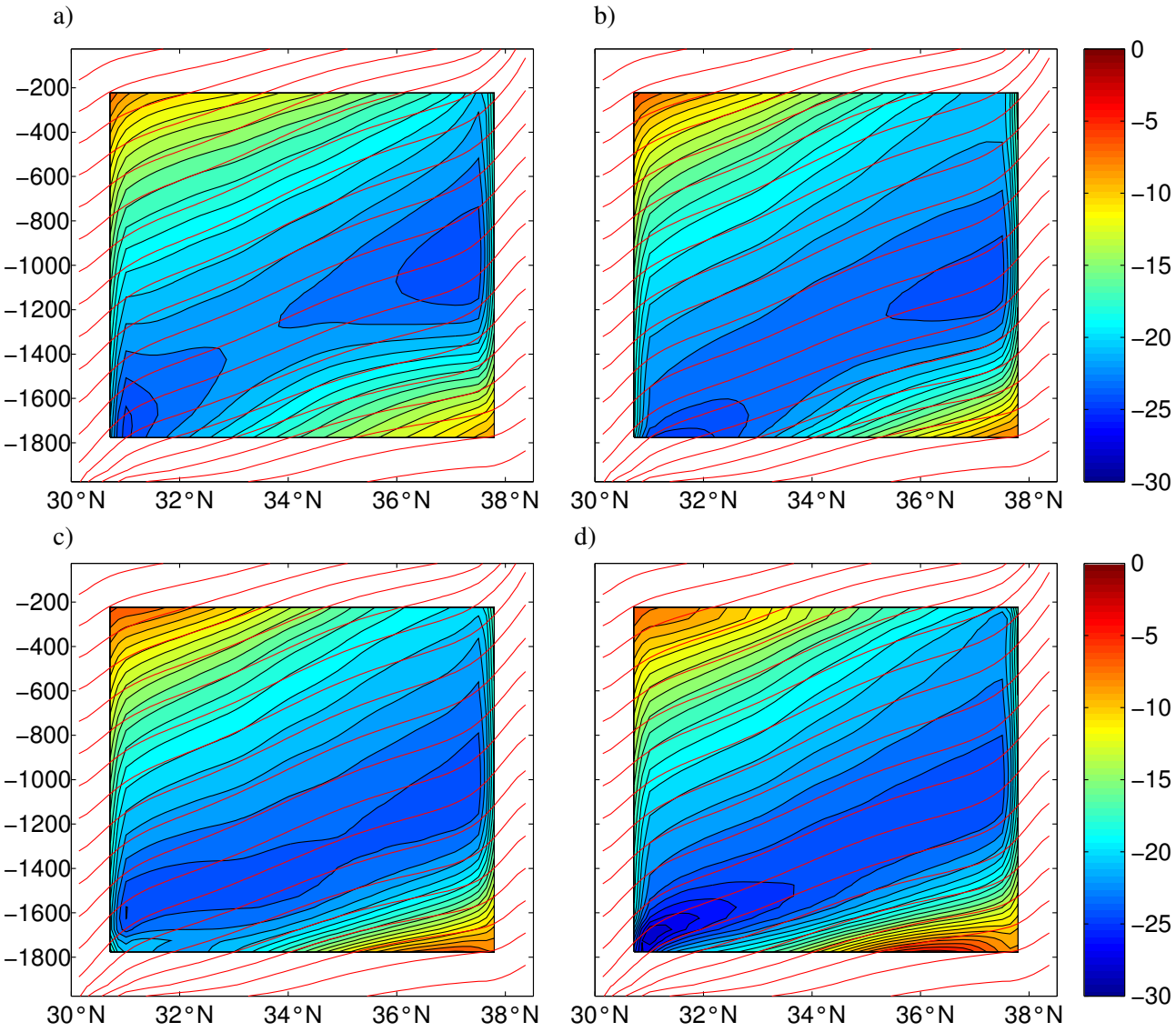

Figure 8: Residual streamfunction in m^2/s in TRM-G calculated to first order (a), second order (b), third order (c) and 4.th order (d). Contour interval is $1\,m^2/s$.